ND70 Series Basaltic Glass Reference Materials for Volatile Element (H_2O , CO_2, S, Cl, F) Measurement and the C Ionisation Efficiency Suppression Effect of Water in Silicate Glasses in SIMS

Yves Moussallam, William Henry Towbin, Terry Plank, Hélène Bureau, Hicham Khodja, Yunbin Guan, Chi Ma, Michael B Baker, Edward M Stolper, Fabian U Naab, et al.

ND70 series basaltic glass reference materials for volatile element (H_2O, CO_2, S, Cl, F) analysis and the C ionization efficiency suppression effect of water in silicate glasses in SIMS analysis.

Yves Moussallam[1], William Henry Towbin[2], Terry Plank[1], Hélène Bureau[3], Hicham Khodja[4], Yunbin Guan[5], Chi Ma[5], Michael B. Baker[5], Edward M. Stolper[5], Fabian U. Naab[6], Brian D. Monteleone[7], Glenn G. Gaetani[7], Kenji Shimizu[8], Takayuki Ushikubo[8], Hyun Joo Lee[1], Shuo Ding[1], Sarah Shi[1], Estelle F. Rose-Koga[9].

[1] *Lamont-Doherty Earth Observatory, Columbia University, New York, USA*

[2] *Gemological Institute of America, 50 W. 47th Street, New York, NY 10036, United States of America*

[3] *IMPMC, Sorbonne Université, CNRS UMR 7590, MNHN, IRD UR 206, 4 place Jussieu, 75252 Paris Cedex 05, France*

[4] *LEEL, NIMBE, CEA, CNRS, Université Paris−Saclay, CEA Saclay, 91191 Gif sur Yvette Cedex, France*

[5] *Division of Geological and Planetary Sciences, California Institute of Technology, Pasadena, California 91125, USA*

[6] *Department of Nuclear Engineering and Radiological Sciences, University of Michigan, Ann Arbor, Michigan 48109, USA*

[7] *Department of Geology and Geophysics, Woods Hole Oceanographic Institution, Woods Hole, MA 02543, USA.*

[8] *Kochi Institute for Core Sample Research, X-star, Japan Agency for Marine-Earth Science and Technology, Monobe-otsu 200, Nankoku, Kochi 783-8502, Japan*

[9] *ISTO, UMR 7327, CNRS-UO-BRGM, 1A rue de la Férollerie, 45071 Orléans cedex 2, France*

Corresponding author: Yves Moussallam; yves.moussallam@ldeo.columbia.edu

Keywords: standards; volatiles; silicate melts; SIMS; ERDA; NRA; FTIR; EMPA

ABSTRACT

We present a new set of reference materials, the ND70-series, for in situ analysis of volatile elements (H_2O, CO_2, S, Cl, F) in silicate glass of basaltic composition. Samples have been synthesised in piston cylinders at pressures of 1 to 1.5 GPa at volatile-undersaturated conditions. They span mass fractions from 0 to 6 wt.% H_2O, from 0 to 1.6 wt.% CO_2 and from 0 to 1 wt.% S, Cl and F. The samples have been characterised by Elastic Recoil Detection Analysis (ERDA) for H_2O, by Nuclear Reaction Analysis (NRA) for CO_2, by Elemental Analyser (EA) for CO_2, by Fourier Transform Infrared Spectroscopy (FTIR) for H_2O and CO_2, by Secondary Ion Mass Spectrometry (SIMS) for H_2O, CO_2, S, Cl and F, and by Electron Microprobe (EMP) for CO_2, S, Cl, and major elements. Comparison between expected and measured volatile amounts across techniques and institutions is excellent. It was found however that SIMS analyses of CO_2 mass fractions using either Cs^+ or O^- primary beams are strongly affected by the glass H_2O content. Reference materials have been made available to users at Ion probe facilities in the US, Europe and Japan. Remaining reference materials are preserved at the Smithsonian National Museum of Natural History where they are freely available on loan to any researcher.

I. INTRODUCTION

Volatile elements (C-O-H-S-Cl-F) play a major role in planetary processes including habitability (e.g., Ehlmann et al., 2016; Foley & Smye, 2018; Dehant et al., 2019), plate tectonics (e.g., Albarède, 2009; Stern, 2018; Nicoli & Ferrero, 2021), mantle melting (e.g., Wyllie, 1971; Eggler, 1976; Dasgupta & Hirschmann, 2006) and volcanic eruptions (e.g., Elskens et al., 1968; Allard, 2010; Edmonds & Woods, 2018). Understanding the planetary-scale cycling of volatiles has hence long been a subject of interest to geoscientists. Critical to that effort is the ability to reliably measure volatiles in geological materials. For volcanologists, igneous petrologists and mantle geochemists, the ability to measure volatile elements in melts (i.e., glasses) and mineral-hosted melt inclusions is of particular interest (e.g., Dixon et al., 1988; Hauri et al., 2002; Métrich & Wallace, 2008). Secondary Ion Mass Spectrometry (SIMS) is a technique that allows for the measurements of all major volatile species in silicate glasses (e.g., Shimizu et al., 2017). One persistent issue with SIMS analyses however is that the ionization efficiency varies by element, primary beam, and major element matrix. To be fully quantitative, the technique requires well characterized reference materials with bulk compositions similar to that of the sample. To date, ion microprobe facilities in Nancy, Paris, Lausanne, Edinburgh, Washington, Woods Hole, Pasadena, Tempe and Kochi, amongst other, have all either acquired or synthesised their own sets of reference material for volatile elements in basaltic glasses. Although sharing natural standards is quite common (e.g., Shimizu et al., 2017), efforts to synthesize large amounts of glasses and to cross-calibrate instruments prior to using the synthetic glasses as standards have been quite limited, particularly on an international scale. This has resulted in significant challenges when attempting to directly compare analytical results generated by different facilities. Furthermore, not all of these facilities possess reference materials that span the entire range of volatile mass fractions found in geological samples. As a consequence, some measurements rely on extrapolation from calibration curves. In this context, we introduce and thoroughly characterize a new series of synthetic basaltic glasses. These glasses are intended to serve as international reference materials for the analysis of H_2O, CO_2, S, Cl, and F mass fractions in natural glasses with a basaltic composition, particularly in the context of SIMS and other micro-beam techniques.

II. EXPERIMENTAL METHOD

We used as starting material a natural Back-Arc-Basin-Basalt, ND-70, dredged at Lat:15º 52' S, Lon:174º51' W from a depth of 2500 m b.s.l. (Keller et al., 2008) at the Mangatolu Triple

Junction in the northern Lau back-arc region (initial composition: 49.2 wt.% SiO_2, 0.8 wt.% TiO_2, 16.1wt.% Al_2O_3, 7.9 wt.% FeO_{tot}, 8.2 wt.% MgO, 12.8 wt.% CaO, 1.9 wt.% Na_2O, 0.15 wt.% K_2O, 0.1 wt.% P_2O_5, 889 ppm S, 219 ppm Cl, 1.02 wt.% H_2O, 76 ppm CO_2, and 148 ppm F; Keller et al., 2008; Caulfield et al., 2012; Lloyd et al., 2013; note that ppm throughout the manuscript refers to $\mu g \cdot g^{-1}$). Five grams of material were crushed, placed in a platinum crucible and fused at 0.1MPa, in air, at 1350 °C for two hours, quenched in water (without submersing the crucible), crushed and mixed again and fused a second time at 1350 °C, 0.1MPa, in air, for an additional two hours and quenched again in water (without submersing the crucible). This volatile-free glass (ND70-degassed) constitutes the first sample in our standard suite (i.e., the blank), and was then used as the starting powder for subsequent piston cylinder experiments.

High-pressure experiments were prepared by adding powdered ND70-degassed glass with the desired amounts of H_2O, CO_2, S, Cl and F in $Au_{80}Pd_{20}$ capsules which were then welded shut. H_2O was loaded as deionized water (using a micro-pipette), CO_2 was loaded as powdered calcite ($CaCO_3$), S was loaded as anhydrite ($CaSO_4$), Cl was loaded as halite (NaCl) and F was loaded as Sellaite (MgF_2). Table 1 gives the intended composition of each experiment based on the added weight of each component (given in Table S1 and totalling 150 to 200mg per experiment). High-pressure experiments were all performed in a piston cylinder apparatus at the Lamont-Doherty Earth Observatory (LDEO). We used a 1/2-inch assembly composed of a CaF_2 pressure cell, a graphite furnace, and MgO sleeves and spacers surrounding the ($Ø_{ext}$ = 5.0 mm, $Ø_{int}$ = 4.8 mm, length = 8.0 mm) $Au_{80}Pd_{20}$ capsule. The temperature was monitored with a D-type ($W_{97}Re_3$-$W_{75}Re_{25}$) thermocouple, separated from the capsule by a 0.8 mm alumina disc. No attempt at controlling oxygen fugacity was made, although given that our starting powder (ND70-degassed) was fused in air, we assume highly oxidised conditions. Run conditions for each experiment are reported in Table 2. Piston cylinder experiments were conducted at pressures of 1 and 1.5 GPa, temperatures of 1225 and 1325°C and equilibrated for 2 h. Experiments were quenched by turning off the electric power and took approximately 5 s to cool bellow 400 °C. An additional experiment, INSOL_MX1_BA4, was run using a powdered mixture of natural basalt (60%) and dacite (30%) (from Kilauea and Tutupaca volcanoes, respectively, Moussallam et al., unpublished) with dolomite (10%) following the same piston cylinder methodology as described above and equilibrated at 1GPa and 1275˚C for 2h. No additional water, S, Cl nor F was added. Initial CO_2 was far above saturation. Finally another experiment VILLA_P2 was run using a powdered mixture of natural basaltic andesite from Villarrica volcano (same starting material as described in Moussallam et al., 2023) to which deionized water, elemental sulfur and oxalic acid dihydrate were added such that the initial mass fractions of CO_2 and S would be above saturation

level (based on previous experiments on similar compositions) at the conditions of the experiment. The charge was run in an internally heated pressure vessel at the American Museum of Natural History and equilibrated at 300 MPa, 1150˚C for 2h at the intrinsic fO_2 of the vessel (~NNO+2; Webster et al., 2011). Both INSOL_MX1_BA4 and VILLA_P2 are not part of the reference material suite that we present here as they were not synthesised in sufficient quantities but were used for calibration purposes during some of the SIMS sessions discussed below. All samples were entirely glassy except ND70-4-01 which partially crystallised on one side of the capsule (the partially crystallized portion was mechanically removed).

III. ANALYTICAL TECHNIQUES

Experiments were analysed by Elastic Recoil Detection Analysis (ERDA) for H_2O, by Nuclear Reaction Analysis (NRA) for CO_2, by Elemental Analyser (EA) for CO_2, by Fourier Transform Infrared Spectroscopy (FTIR) for H_2O and CO_2, by Secondary Ion Mass Spectrometry (SIMS) for H_2O, CO_2, S, Cl and F, and by Electron Microprobe (EMP) for CO_2, S, Cl and major elements.

a) Nuclear Microprobe (ERDA and NRA)

H_2O and CO_2 absolute mass fractions were evaluated using two Ion Beam Analysis techniques, namely Elastic Recoil Detection Analysis (ERDA) and Nuclear Reaction Analysis (NRA). Measurements were performed at the Laboratoire d'Etude des Eléments Légers (LEEL) joint CEA-CNRS laboratory in Saclay (Khodja et al., 2001) where these techniques are regularly employed to quantify light elements in various materials, including geological samples (Clesi et al., 2018; Malavergne et al., 2019). H_2O was analysed as H by ERDA following the approaches described in Bureau et al. (2009). We used a $^4He^+$ ion beam at 2.7 MeV energy that interacts with the samples at grazing incidence. A 12 μm Mylar absorber was mounted between the sample and the forward (30°) particle detector to stop all scattered $^4He^+$ and let recoil H^+ ions reach the detector. The CO_2 was analysed as C by NRA, making use of the sensitive $^{12}C(d,p)^{13}C$ nuclear reaction at 170° detection angle using a deuteron ($^2H^+$) microbeam at 1.4 MeV. Although no absorber was used, detected protons, in the 2750–3150 keV energy range, are far above backscattered deuterons. Quantification was performed by precisely measuring detector solid angles using reference materials and by adjusting experimental spectra with the SIMNRA software (Mayer, 1999). The parasitic

contribution from the $^{28}Si(d,p)^{29}Si$ was systematically subtracted using a Suprasil reference spectrum (H_2O<1 ppm; e.g., Shimizu et al., 2019).

b) Elemental Analyser

We used a Costech elemental analyzer (ECS4010) at the Lamont−Doherty Earth Observatory to measure CO_2 (as C) in the two most CO_2-rich experiments (with > 1 wt% CO_2). Hand-picked glass samples were precisely weighed on a microbalance with a precision of ± 0.001 mg, and then wrapped in 3.2×4 mm tin foil envelopes. 18.253 mg were used for sample ND70-5-02 and 12.636 mg were used for sample ND70-6-02. These encapsulated samples were subjected to combustion (at ~1700 °C) over a chromium (III) oxide catalyst with excess oxygen (25 mL/min). The carrier gas was helium, flowing at a rate of 100 mL/min. To ensure complete oxidation of sample carbon into CO_2 and the elimination of remaining halogens or sulfur, silvered cobaltous/cobaltic oxide, positioned lower in the quartz combustion tube, was used. The analyser was calibrated directly prior to sample analysis using mixtures of oxalic acid and SiO_2 with 1, 2, 5, 20, and 70 wt% of CO_2. This calibration (R^2 = 0.9999; Fig. S1) was then used to determine the CO_2 content of the samples. Error on C was estimated at ±2% (±7.3% on CO_2) based on reproducibility of external standards (calcite and dolomite) similar to other studies using an elemental analyser for silicate glasses (e.g., Moussallam et al., 2015, 2016).

c) Fourier Transform Infrared Spectroscopy (FTIR)

H_2O and CO_2 mass fractions in doubly polished experimental glasses were measured using a N_2 purged Thermo Scientific Nicolet iN10 mx Fourier Transform Infrared Spectrometer (FTIR) at LDEO. Measurements were collected with aperture sizes varying between 100 × 100 μm and 200 × 200 μm. Thickness of the doubly polished wafers were measured using a digital micrometer (Mitutoyo Digimatic Indicator) and calculated using the "interference fringe" method (Tamic et al., 2001) that requires determining the wavelength of interference fringes of reflectance spectra collected from the sample. The latter method enables determining the thickness at the same spot where the transmission spectra is collected. Several spots were measured on each glass to ensure no heterogeneity. Baseline fitting, density calculations, absorption coefficients and ultimately H_2O and CO_2 concentration were determined using PyIRoGlass (Shi et al., 2023; https://github.com/sarahshi/PyIRoGlass), except for INSOL_MX1_BA4 where we used the spectra obtained from a de-volatised (i.e., fused twice at 0.1MPa in air for 2h) version of the same composition to define the baseline.

d) Secondary Ion Mass Spectrometry at CNRS-Nancy

A first indium mount containing all the experimental glasses was cleaned with DI and Millipore filtered water, dried and then coated with a ~20 nm Au layer. Volatile (H_2O, CO_2, Cl, F, S) contents in experimental glasses were determined using a Cameca IMS 1280 ion microprobe at CRPG-CNRS-Nancy, France. We used a 20 kV (10 kV for the ion acceleration at the source and 10 kV for ion extraction at the sample surface) Cs^+ primary beam with a current of 1 nA. A –10 kV electron flood gun was applied at the sample surface to charge compensate the positive Cs^+ ion surface implantation. During analysis (with e-gun on), the sample potential is held at –5 kV and the electron gun is operated at –5 kV, so that electrons arrive at the sample surface with near-zero energy. A 180 s pre-sputter with a 30 × 30 µm square raster was applied, then analyses were collected on the 15 to 20 µm spot in the center of the rastered area using a mechanical aperture placed at the secondary ion image plane. Analyses were performed in multi-collector mode; CO_2, H_2O, F, Cl and S were measured using an electron multiplier, while Si and O were measured on a faraday cup. We collected signals for ^{12}C (8 s), ^{17}O (3 s), $^{16}O^1H$ (6 s), ^{18}O (3 s), ^{19}F (4 s), ^{27}Al (3 s), ^{30}Si (3 s), ^{32}S (4 s) and ^{35}Cl (6 s; counting times in parentheses), with 2 s waiting time after each switch of the magnet. This cycle was repeated 10 times during one analysis for a total analysis duration of 12 minutes. The mass resolution of ~7000 (with the contrast aperture at 400 µm, the energy aperture at 40 eV, the entrance slit at 52 µm and the exit slit at 173 µm) meant that complete discrimination of the following mass interferences was achieved: $^{34}S^1H$ on ^{35}Cl; ^{17}O on $^{16}O^1H$; $^{29}Si^1H$ on ^{30}Si; $^{31}P^1H$ on ^{32}S.

Together with our experimental glasses, we measured natural and experimental basaltic glasses KL2G (Jochum et al. 2006) KE12 (Mosbah et al. 1991), VG2 (Jarosewich et al. 1980), experimental glasses N72, M34, M35, M40, M43 and M48 (Shishkina et al. 2010), and the Macquarie glasses 40428 and 47963 (Kamenetsky et al. 2000) under the same analytical conditions at the beginning and end of the session. The Calibration lines are shown in Fig. S2 to S6. All existing standard values are reported in Table S2.

e) Secondary Ion Mass Spectrometry at Woods Hole Oceanographic Institution

A second indium mount containing a different set of chips of the experimental glasses, was cleaned with DI and Millipore filtered water, dried and then coated with a ~20 nm Au layer. Volatile concentration analyses were conducted on a Cameca IMS1280 at the Northeast National Ion Microprobe Facility (NENIMF) at the Woods Hole Oceanographic Institution.

The standards were measured in separate sessions using a $^{133}Cs^{+}$ primary beam, then a $^{16}O^{-}$ primary beam. The calibration lines are shown in Fig. S2 to S7.

Cs SIMS measurements:

A 500pA to 1nA $^{133}Cs^{+}$ primary ion beam, accelerated 10kV, was focused to a 10–15 µm diameter, then rastered to produce a ~25 × 25 µm crater. Secondary ions ($^{12}C^{-}$, $^{16}OH^{-}$, $^{18}O^{-}$, $^{19}F^{-}$, $^{30}Si^{-}$, $^{31}P^{-}$, $^{32}S^{-}$ and $^{35}Cl^{-}$) were extracted with a 10kV voltage potential. The extracted and magnified secondary ions were centered through a 600 × 600 µm mechanical field aperture, which blocked transmission of secondary ions from outside of the central ~7.5 × 7.5 μm^2 of the crater. The secondary field aperture is necessary to minimize the transmission of background and surficial volatile ions residing in the sample chamber, the surrounding sample surface, and within the outer edges of the sputtered crater. A normal-incidence electron gun set at –10kV was used to compensate for positive charge buildup within the sample crater. The energy bandwidth for the secondary ions was ~60 eV. A mass resolving power > 5500 was used to separate interfering masses, such as $^{17}O^{-}$ from $^{16}OH^{-}$. Each measurement consisted of 180 seconds of presputtering, automatic secondary beam centering, and automatic mass calibration, followed by five cycles of counting of each ion intensity on an ETP electron multiplier in magnet peak jumping mode. Count times in seconds for each mass were as follows: $^{12}C^{-}$ = 10, $^{16}OH^{-}$ = 5, $^{18}O^{-}$ = 3, $^{19}F^{-}$ = 5, $^{30}Si^{-}$ = 3, $^{31}P^{-}$ = 5, $^{32}S^{-}$ = 5, $^{35}Cl^{-}$ = 5. Background intensities were measured on Suprasil 3002 glass for C, OH, F, P, and S, and on Herasil glass for Cl.

O^{-} SIMS measurements:

A 10nA $^{16}O^{-}$ primary ion beam, accelerated 13kV, was focused to a ~25 µm diameter, then rastered to produce a ~30 to 35 µm diameter crater. Secondary ions ($^{12}C^{+}$, $^{16}O^{+}$, $^{16}OH^{+}$, $^{19}F^{+}$, $^{30}Si^{+}$, $^{31}P^{+}$, $^{32}S^{+}$ and $^{35}Cl^{+}$) were extracted with a 10kV voltage potential. A 1250 × 1250 µm mechanical field aperture was set to blocked transmission of secondary ions from outside of the central ~15 × 15 µm the measurement crater. The energy bandwidth for the secondary ions was ~50 eV. A mass resolving power > 5500 was used to separate interfering masses, such as $^{17}O^{+}$ from $^{16}OH^{+}$. Each measurement consisted of 120 seconds of presputtering, automatic secondary beam centering, and automatic mass calibration, followed by five cycles of counting of each ion intensity on an ETP electron multiplier in magnet peak jumping mode. Count times in seconds for each mass were as follows: $^{12}C^{+}$ = 5, $^{16}O^{+}$ = 3, $^{16}OH^{+}$ = 5,

$^{19}F^{+}$ =_5, $^{30}Si^{-}$ = 2, $^{31}P^{+}$ = 5, $^{32}S^{+}$ = 5, $^{35}Cl^{+}$ = 5. Background intensities were measured on Suprasil 3002 glass for C, OH, F, P, and S, and on Herasil glass for Cl.

f) Secondary Ion Mass Spectrometry at Caltech

Volatile concentration analyses were conducted on a Cameca ims-7f GEO instrument at the Caltech Microanalysis Center on the second indium mount. The standards were first measured with a Cs^{+} beam, and later with an $^{16}O^{-}$ beam. The calibration lines are shown in Fig. S2 to S7.

Cs^{+} SIMS measurements:

A 10 kV Cs^{+} primary ion beam of ~3–4 nA (~15 um in diameter) was used to sputter the samples and produce secondary ions. The beam was rastered to produce craters ~25 × 25 μm in dimension, and a 100 μm field aperture was used to enable only the ions from the central 8 μm of the craters to be transmitted for detection. Possible edge effects were further eliminated with electronic gating (36% in area). Secondary ions ($^{12}C^{-}$, $^{16}OH^{-}$, $^{18}O^{-}$, $^{19}F^{-}$, $^{30}Si^{-}$, $^{31}P^{-}$, $^{32}S^{-}$ and $^{35}Cl^{-}$) of –9 keV were collected with an electron multiplier (EM) in the peak-jumping mode. Each measurement consisted of 120 s pre-sputtering, followed by automated secondary beam alignment, peak centering, and 20 cycles of data collection. The counting time of each mass was 1 s per cycle. The energy bandwidth for the secondary ions was set at ~45 eV. Sample charging compensation was provided by a normal-incidence electron gun NEG at –9 kV. A mass resolving power (MRP) of ~5000 was used to remove any significant interferences to the masses of interest (e.g., $^{17}O^{-}$ from the $^{16}OH^{-}$ peak). Data were corrected for EM background and deadtime. The instrumental volatile backgrounds were checked with the Suprasil 3002 glass.

O^{-} SIMS measurements:

For this SIMS setup, a focused $^{16}O^{-}$ primary beam of –13 kV and ~8 nA was used to sputter areas of 25 × 25 μm for analysis. Positive secondary ions of $^{1}H^{+}$, $^{12}C^{+}$, and $^{28}Si^{+}$ of +8.5 kV were collected in the peak-jumping mode with an EM (for $^{1}H^{+}$, $^{12}C^{+}$) or a Faraday cup (FC, for $^{28}Si^{+}$). Each measurement consisted of 20 cycles of counting of $^{1}H^{+}$ (1s), $^{12}C^{+}$ (3s), and $^{28}Si^{+}$ (1s). Because there were no significant interferences to the masses of interest, the mass spectrometer was operated at low mass resolution conditions (MRP ~1800). Minimal sample charging was corrected with automatic scan and adjustment of the sample high voltage during

measurement. The other analytical parameters and operation were similar to those used for the Cs^+ session. The C and H backgrounds were checked with Suprasil for this O^- session, which yielded $^{1}H^{+}/^{28}Si^{+}$ = 3.7E–5 and $^{12}C^{+}/^{28}Si^{+}$ = 2.1E–7. Such backgrounds were insignificant to the measured CO_2 and H_2O concentrations in this set of standards. Nevertheless, the reported results were corrected for this background.

g) Secondary Ion Mass Spectrometry at JAMSTEC-Kochi

All the experimental glasses were polished and embedded in a third, indium-filled aluminium disc together with an internal standard basaltic glass of EPR-G3. After cleaning by acetone and de-ionized water, the sample mount was dried in a vacuum oven for a day and then coated with ~30 nm Au. Volatile (H_2O, CO_2, Cl, F, S) contents in the experimental glasses were determined using a Cameca IMS 1280 ion microprobe at Kochi Institute, JAMSTEC, Japan, following the method of Shimizu et al. (2017). We used a 10 to 15 μm diameter Cs^+ primary beam with a current of ~0.5 nA and an electron gun to compensate for charge build-up at the sample surface. The field aperture size was set at 1 × 1 mm corresponding to 5 × 5 μm of the field of view of the secondary ion image in order to collect signals from the centre of the analysis spot to avoid surface contamination near the beam edge. Mass resolving power of ~6000 was applied for separating interference signals. Analyses were performed by a magnetic peak switching method. Secondary ion signals of ^{12}C (3s counting time), ^{16}OH (1s), ^{19}F (1s), ^{30}Si (1s), ^{31}P (1s), ^{32}S (1s) and ^{35}Cl (1s) were detected by an axial electron multiplier (there was a 2s waiting time after each switch of the magnet). Each analysis consisted of 20s for pre-sputtering, 120s for auto-centering of secondary ions to the field and contrast apertures and 10 cycles of measurements. The total measurement duration for each analysis was ~7 mins. To evaluate the volatile contents of the experimental glasses, we used in-house synthetic and natural silicate standard glasses described in Shimizu et al. (2017). The volatile contents of these in-house standards were determined by FTIR (H_2O and CO_2 contents) and pyrohydrolysis-ion chromatography (F, Cl and S contents) (Shimizu et al., 2015). Calibration lines are show in Fig. S2 to S7.

h) Electron Microprobe at Caltech

Carbon contents of the glass samples ND70-3-01, ND70-4-02, ND70-5-02, and ND70-6-02 as well as the following secondary standards: five gem-quality scapolites (from Prof. George Rossman), a natural spurrite (from the Caltech mineral collection; CIT-11435; Joesten, 1974), and a eutectic glass composition in the CaO-Al_2O_3-SiO_2 (CAS) system were analyzed at

Caltech using a JEOL JXA-iHP200F field-emission electron microprobe in WDS mode, interfaced with the Probe for EPMA software from Probe Software, Inc. The secondary standards were carefully polished down to a ¼ μm finish and ultrasonicated in ethanol; the scapolites were mounted in indium while the spurrite and CAS glass were mounted in epoxy (the ND-series glasses were prepared at Lamont). Just prior to the start of the analytical session, the ND-series glasses, secondary standards, and primary standards were plasma cleaned using an Evactron system to remove hydrocarbon contamination on their surfaces and then coated with an ~1-nm layer of Ir (Armstrong & Crispin, 2013) using a Cressington 208HR sputter coater (all samples were coated at the same time). Analytical conditions were 10 kV and 15 kV accelerating voltages, a 50 nA beam current, and a 10 μm defocused beam. The LDE2 crystal was used for carbon analysis and counting times were 60 s on peak and 30 s on each background. The on-peak O interference with the C peak, revealed by WDS scans of the glass samples, was corrected using the Probe for EPMA program. Cohenite (Fe_3C; C$K\alpha$) from the iron meteorite Canyon Diablo and Elba hematite (O$K\alpha$; for the C on-peak interference correction) were used as primary standards. Each ND-series glass and secondary standard was analyzed five times. Quantitative carbon analyses were processed with the CITZAF matrix correction procedure (Armstrong, 1995) using the major and minor element composition of each phase.

For the secondary standards, the CO_2 contents of the five gem-quality scapolites were determined using NRA at the Michigan Ion Beam Laboratory at the University of Michigan using a deuteron beam energy of 1.35 MeV and procedures described in Hammerli et al. (2021). The measured CO_2 contents ranged from 0.70 to 3.57 wt.%. The CAS eutectic glass was fused at 1-atm in air and is assumed to have a CO_2 content of zero (the extremely low solubility of CO_2 in basalts and more silica-rich compositions at pCO_2 = 1 bar, and the very low mole fraction of CO_2 in air support this assumption e.g., Blank, 1993; Stolper & Holloway, 1988). The CO_2 content of the spurrite was calculated from stoichiometry, i.e., the wt.% CO_2 was adjusted until the cation sum of C and B (on the basis of 11 oxygens) was equal to 1 (the boron content was determined by SIMS using the Cameca IMS 7f-GEO at Caltech; see Krzhizhanovskaya et al., 2023 for a discussion of B- and S-bearing spurrite). The calculated CO_2 content (9.36 wt.%), plus the B_2O_3 content determined by SIMS, plus the remaining oxide concentrations determined by EMPA resulted in an oxide sum of 100.06

wt.%. We used this stoichiometric approach because the abundant small inclusions on the surface of the polished spurrite sample precluded determining its C content by NRA.

Supplemental Fig. S8 compares the measured EMP CO_2 contents of the secondary standards with their accepted values and shows that the probe analyses are systematically low and offset from the solid 1:1 line. The dashed line, an unweighted least-squares fit to the seven secondary standards, has an R^2-value of 0.998. The fact that the best-fit line doesn't go through the origin most likely reflects an over-correction of the oxygen interference with the carbon peak. We assumed that the EMP carbon analyses for the ND-series glasses were similarly offset from their "true" values, and we used the dashed-best-fit line to adjust their CO_2 contents, i.e., to project them onto the y-axis in Fig. S8. It is these projected ND-series CO_2 concentrations that are plotted in Fig. 2 and listed in Table 4.

i) Electron Microprobe at AMNH

The S, Cl and major element compositions were measured with a Cameca SX5-Tactis at the American Museum of Natural History on a new set of polished glasses mounted in resin. We used an accelerating voltage of 15 kV, a defocused beam of 10 µm, a beam current of 4 nA for Na (with 10s count time), 10 nA for Mg, Al, Si, Ca (20s count time), P, K, Ti, Mn, Fe (30s count time), and 40 nA for S and Cl (70s and 40s count times respectively). Na was analysed first to minimize Na loss during analysis. The instrument was calibrated on natural and synthetic mineral standards and glasses: albite (Na), olivine (Mg), potassium-feldspar (Al, Si and K), berlinite (P), anorthite (Ca), rutile (Ti), rhodonite (Mn), fayalite (Fe), barium sulfate (S) and scapolite (Cl). Errors (two standard deviation) are ±0.43 for SiO_2, ±0.18 for Na_2O, ±0.02 for K_2O, ±0.17 for Al_2O_3, ±0.36 for CaO, ±0.24 for FeO, ±0.11 for MgO, ±0.04 for TiO_2, ±0.05 for MnO, ±0.04 for P_2O_5, ±0.01 for S and ±0.03 for Cl.

IV. RESULTS

Here we compare results of the different analytical methods against the mass fractions calculated from the quantities loaded into the experimental capsules. Loaded mass fractions are used as a starting point for comparisons with no assumption that they might represent "correct" values. Results from EMPA analyses are given in Table 3, results from ERDA, NRA, FTIR and EA are given in Table 4 and results from SIMS are given in Table 5. Raw SIMS results are given in Tables S3 to S7. SIMS calibration lines are shown in Fig. S2 to S7.

FTIR spectra and deconvolutions are shown in Fig. S9. Raw FTIR spectra are given in Moussallam (2024a). Raw NRA spectra are given in Moussallam (2024b).

a) H_2O

Water in the new reference glasses was analysed by ERDA, FTIR and at the ion microprobe facilities at CRPG-CNRS-Nancy, WHOI, Caltech and JAMSTEC-Kochi. Figure 1 compares the water contents measured by all of these techniques with the expected (i.e., loaded) values. The agreement is in most cases excellent (better than 8%). Significant deviation from the one-to-one line is found for one Caltech Cs^+ beam SIMS analysis of sample ND70-4-02 although the discrepancy between loaded and measure H_2O content in ND70-4-02 disappears if the measured $^{16}O^1H/^{18}O$ ratio is used instead of the $^{16}O^1H/^{30}Si$ ratio. Significant deviation from the one-to-one lines is also found for the Kochi Cs^+ beam SIMS analyses of sample ND70-5-02 and ND70-6-02. Note that these two samples have concentrations that require very significant extrapolation of the calibration line (Fig. S2). Caltech O^- beam SIMS analyses are not shown as most unknown glasses had values outside the calibration range for that session.

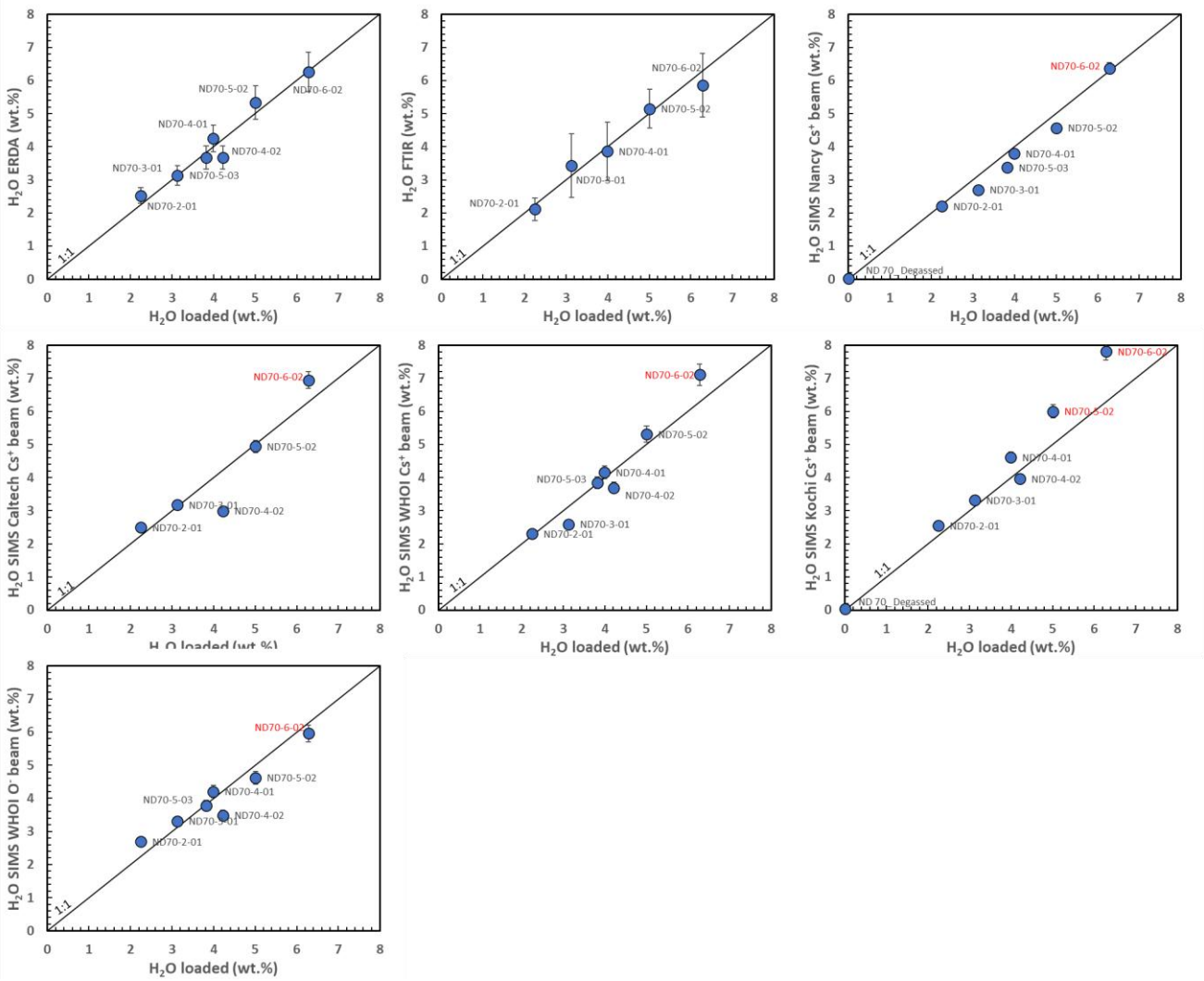

***Figure 1**: Comparison between the expected (i.e., loaded) and measured water content in the new reference materials. Samples labelled in red were measured outside their respective calibration ranges (Fig. S2).*

400
401 **b) Carbon dioxide**

402 CO_2 in the new reference glasses was analysed by NRA, EA, FTIR, EMPA and at the ion
403 microprobe facilities at CRPG-CNRS-Nancy, WHOI, Caltech and JAMSTEC-Kochi. Figure
404 2 compares the CO_2 contents measured by all these techniques with the expected (i.e.,
405 loaded) values. Sample ND70_Degassed was measured by SIMS at CRPG-CNRS-Nancy and
406 JAMSTEC-Kochi. We found that the sample provides a good "blank" for CO_2 with $^{12}C/^{30}Si$
407 signals comparable to those obtained on pure quartz and San Carlos olivine (Table S8).
408 Figure 2 shows that samples ND70-2-01, ND70-3-01, ND70-4-01, ND70-4-02 and ND70-5-
409 03 have measured CO_2 contents significantly higher than expected based on the loaded
410 amounts of CO_2 (although not all five samples were analysed using all of the techniques or
411 ion probes). For sample ND70-5-02, measured CO_2 contents from NRA and EA analyses
412 were significantly higher than the loaded (i.e., expected) CO_2 concentration. In contrast, EMP
413 analyses, O^- beam SIMS analyses from Caltech and WHOI and Cs^+ beam SIMS analyses
414 from JAMSTEC-Kochi were close to the expected concentration, while Cs^+ beam SIMS
415 analyses at CRPG-CNRS-Nancy, WHOI and Caltech yielded significantly lower
416 concentrations. The measured CO_2 content of sample ND70-6-02 by NRA is higher than the
417 amount loaded, close to the expected amount when using EA and FTIR, but significantly
418 lower than the amount loaded when considering EMPA and all SIMS analyses (regardless of
419 primary species). The mismatch between loaded and measured CO_2 contents in most
420 experiments may reflect C contamination either during sample preparation or during the
421 experiment. C diffusion through platinum capsules has been documented by Brooker et al.,
422 (1998) at temperatures around 1650°C, significantly higher than the temperatures used here
423 and no "blackening" of our glasses was observed.

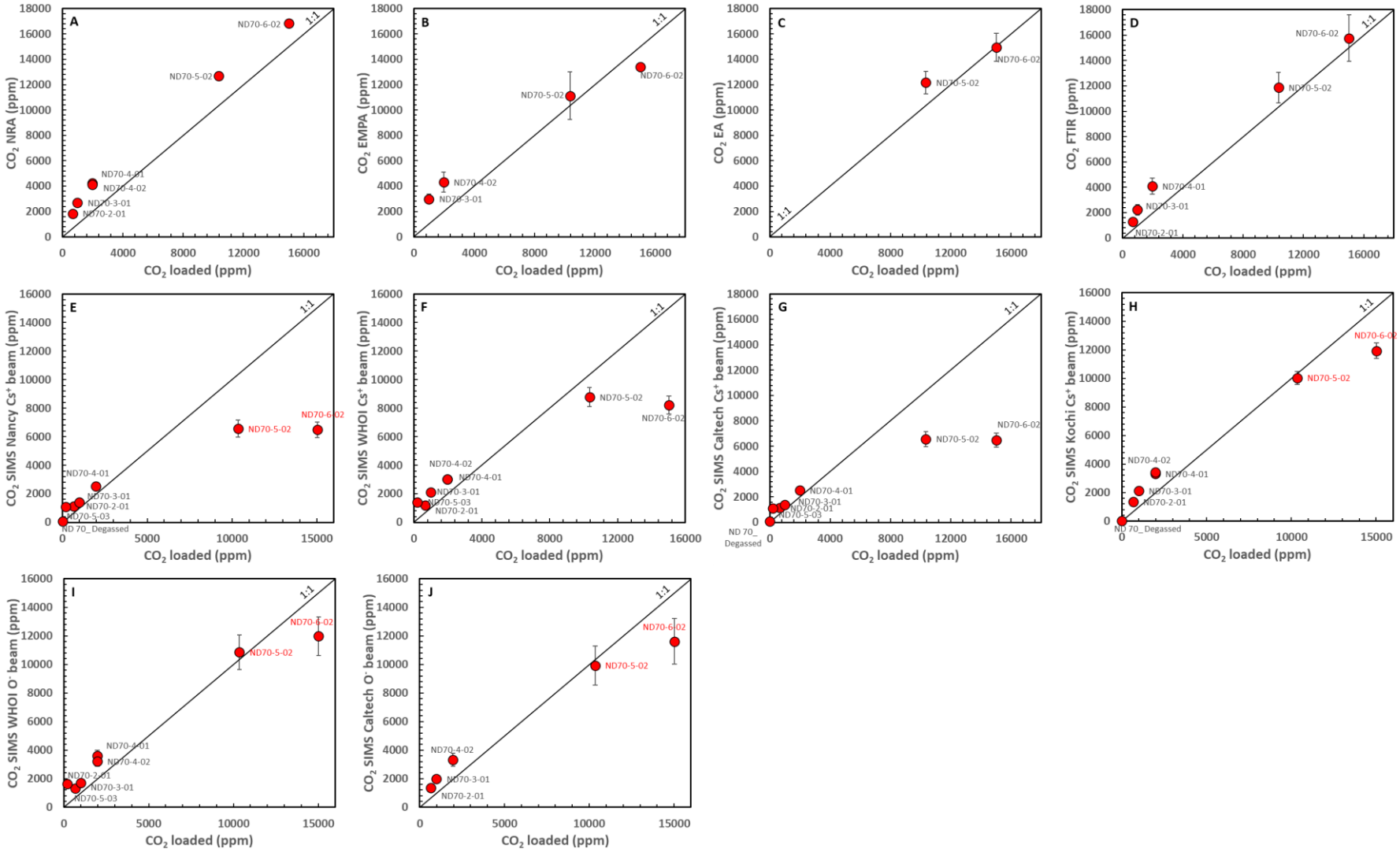

***Figure 2**: Comparison between the expected (i.e., loaded) and measured CO_2 content in the new reference materials. Samples labelled in red were measured outside their respective calibration ranges (Fig. S3 and S7).*

c) Sulfur

S in the new reference glasses was analysed by EMP at AMNH and at the ion microprobe facilities at CRPG-CNRS-Nancy, WHOI, Caltech and JAMSTEC-Kochi. Figure 3 compares the loaded S contents with the mass fractions measured by EMP and the four ion probes. The agreement is excellent for samples ND70_Degassed, ND70-2-01, ND70-3-01, ND70-5-03 and, except for the Kochi analyses, ND70-5-02. Samples ND70-4-01 and ND70-4-02 show somewhat lower than expected values in the Caltech and WHOI SIMS analyses. Compared to the loaded concentration, the measured S content in sample ND70-6-02 was significantly lower in the EMP and Caltech and WHOI SIMS analyses and higher in the Nancy and Kochi SIMS analyses. Note that the SIMS S measurements for both ND70-5-02 and ND70-6-02 are based on very significant extrapolation from calibration ranges (Fig. S4).

d) Chlorine

Chlorine in the new reference glasses was analysed by EMP at AMNH and at the ion microprobe facilities at CRPG-CNRS-Nancy, WHOI, Caltech and JAMSTEC-Kochi (the Caltech analyses are not shown as most of the unknown glasses had values outside the calibration range for that session). Figure 4 compares the Cl contents measured by these techniques with the expected (i.e., loaded) values. Samples ND70_Degassed, ND70-2-01, ND70-3-01, ND70-4-01, ND70-4-02 and ND70-5-03 all show good to excellent agreements. The measured Cl contents in samples ND70-5-02 and ND70-6-02 are significantly higher than loaded amounts in all three sets of SIMS analyses and in the EMP analyses. Note that the SIMS Cl measurements for both ND70-5-02 and ND70-6-02 are based on very significant extrapolation from calibration ranges (Fig. S5).

e) Fluorine

Fluorine in the new reference glasses was analysed at the ion microprobe facilities at CRPG-CNRS-Nancy, WHOI, JAMSTEC-Kochi and Caltech but Caltech analyses are not shown as most of the unknown glasses had F mass fractions outside the calibration range for that session. Figure 5 compares the F contents measured by the Nancy, WHOI and Kochi ion probes with the expected (i.e., loaded) values. Samples ND70_Degassed, ND70-2-01, ND70-3-01, ND70-4-01, ND70-4-02 and ND70-5-03 all show good to excellent agreements between the measured and expected mass fractions. For samples ND70-5-02 and ND70-6-02 where measurements are based on very significant extrapolation from calibration ranges (Fig.

S6) the agreement is excellent for the Nancy and WHOI SIMS analyses but the Kochi analyses for these glasses are significantly higher.

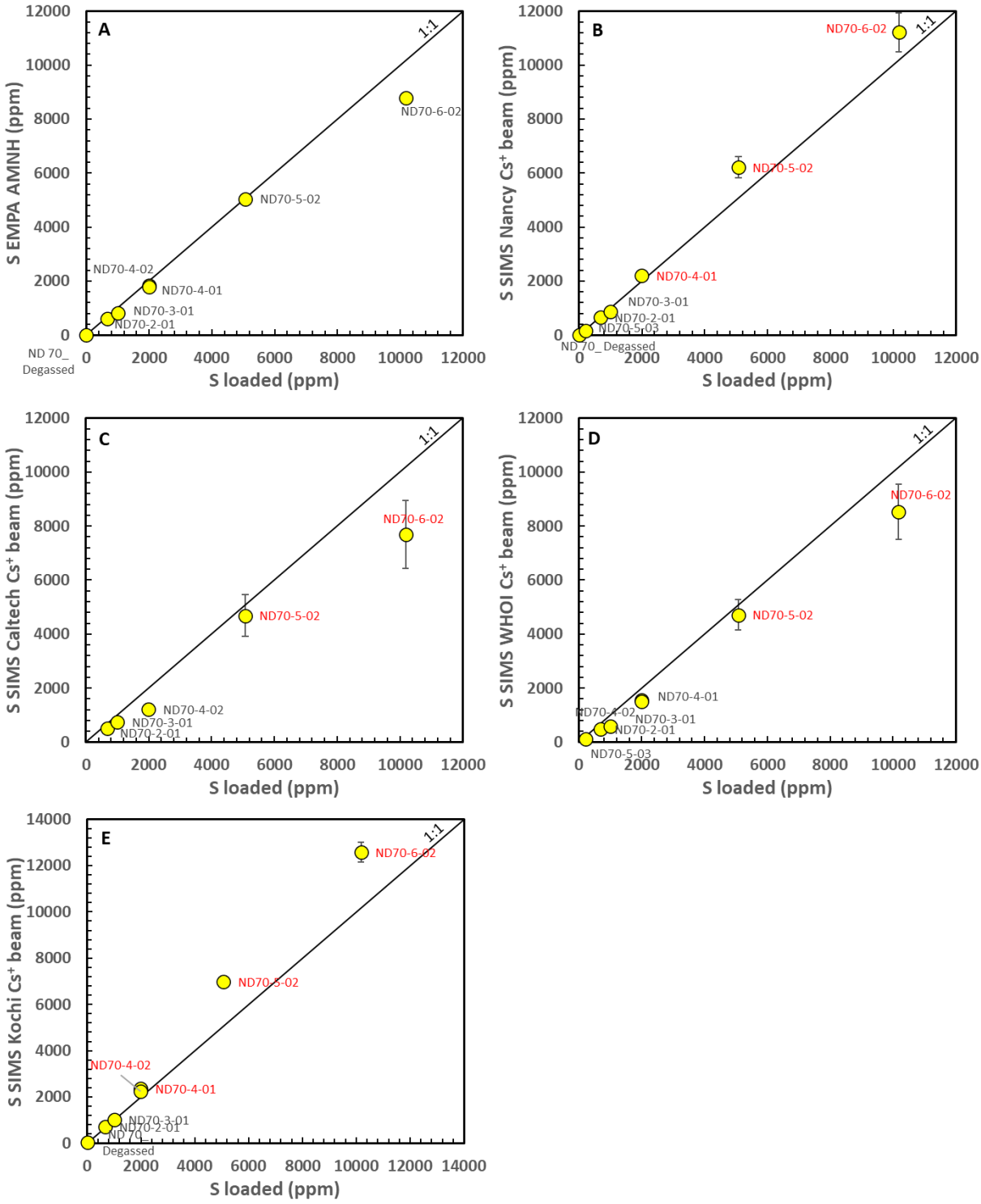

Figure 3*: Comparison between the expected (i.e., loaded) and measured S content in the new reference materials. Samples labelled in red were measured outside their respective calibration ranges (Fig. S4).*

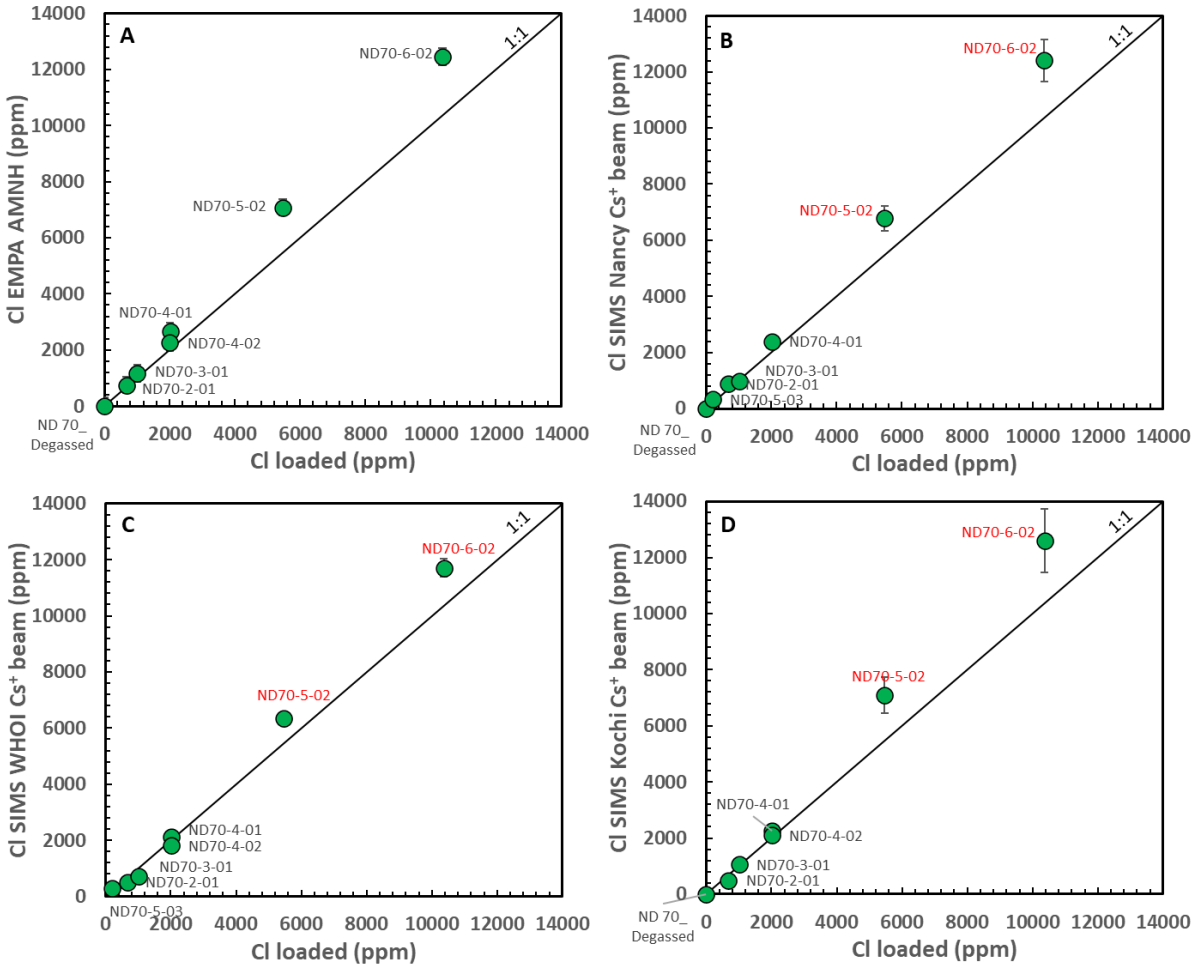

***Figure 4**: Comparison between the expected (i.e., loaded) and measured Cl content in the new reference materials. Samples labelled in red were measured outside their respective calibration ranges (Fig. S5).*

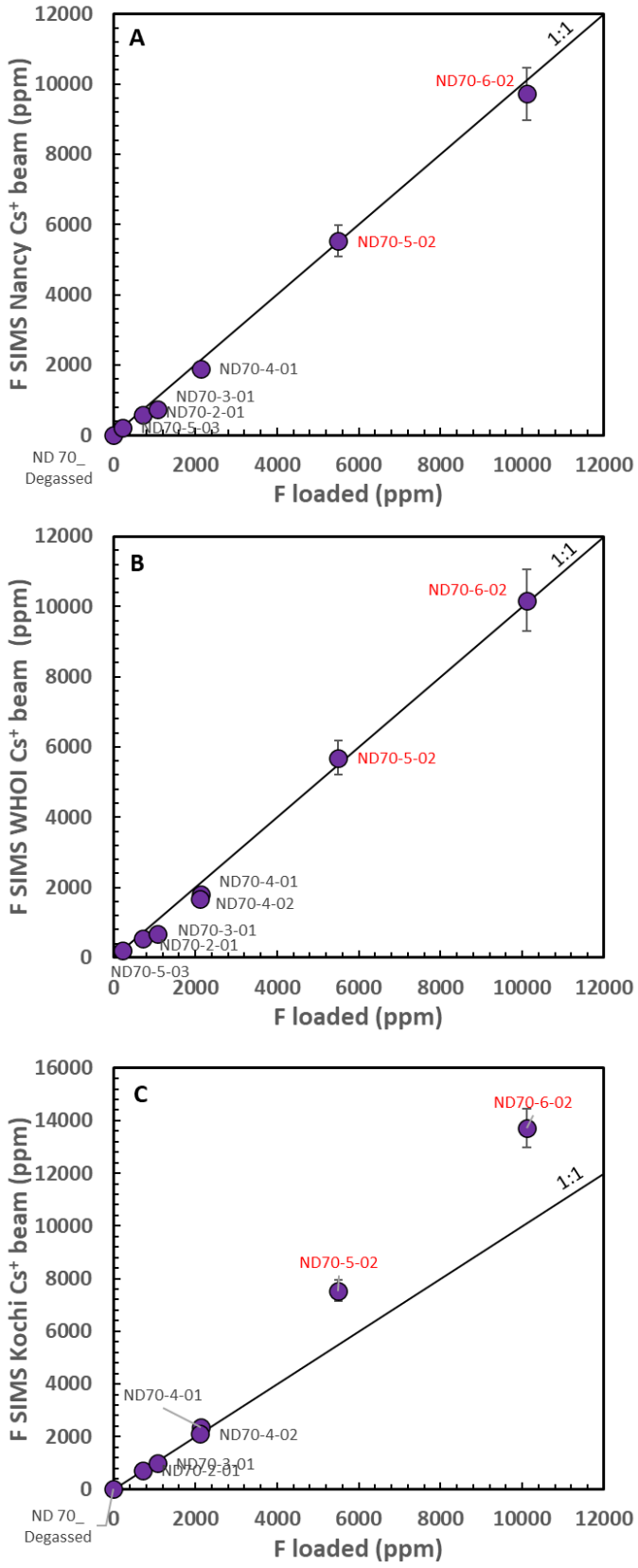

Figure 5*: Comparison between the expected (i.e., loaded) and measured F content in the new reference materials. Samples labelled in red were measured outside their respective calibration ranges (Fig. S6).*

476

477 **f) Reference material homogeneity**

478 Based on volatile solubility experiments described in the literature (e.g., Stolper & Holloway,
479 1988; Blank & Brooker, 1994; Lesne et al., 2011; Iacono-Marziano et al., 2012; Moussallam,
480 et al., 2015; Allison et al., 2019) our experimental durations and temperatures should have
481 been sufficient to achieve homogeneity in term of both major and volatile element
482 distributions in the experimental glasses (recall that the starting material was a twice-fused
483 glass). Evidence of homogeneity is further provided by the good inter-instrument comparison
484 (see following section). Excepted for the WHOI and Caltech SIMS analyses which were
485 performed on the same mount (i.e., the same pieces of glass), all other techniques were
486 performed on distinct sets of glasses.

V. DISCUSSION

a) Inter-instrument comparison

Figure 6 compares the mean absolute deviation (i.e., $\frac{\sum normalized(|\Delta|)}{n}$, in %) between all the techniques used to measure H_2O, CO_2, S, Cl and F contents in the ND70 suite, and Fig. 7 graphically compares all the measurements. For H_2O, results from ERDA, FTIR and five SIMS sessions all agree with average mean absolute deviations around 10% between methods. The JAMSTEC-Kochi SIMS results show larger deviations (15% on average) but this is entirely due to samples ND70-5-02 and ND70-6-02 being outside the calibration range for that SIMS session. For CO_2, NRA, EA, FTIR and EMPA analyses agree on average within ±9%. Cs^+ primary beam SIMS analyses at Caltech, WHOI and Nancy agree reasonably well with each other (on average within ±18%) but agree poorly with the other techniques due to the low values measured in samples ND70-5-02 and ND70-6-02, which were outside the calibration range for the Nancy SIMS session and dominate the mean absolute deviation calculation (more on this in the following section). Cs^+ primary beam SIMS analyses at Kochi however agrees with O^- primary beam SIMS analyses at Caltech and WHOI (on average within ±5%) and agrees poorly with the other Cs^+ primary beam SIMS analyses (on average within ±33%). O^- primary beam SIMS analyses at Caltech and WHOI agree with each other within ±6% and are in reasonable agreement with the results from NRA, EA and FTIR, on average within ±19%, but differ from the EMPA mass fractions by, on average, ±27%. Note that only two samples were analysed by EA, partially explaining why this technique shows the lowest average mean absolute deviation.

For S, the averages of the EMP analyses and the four sets of Cs^+ primary beam SIMS analyses (Caltech, WHOI, Kochi and Nancy) all agree within approximately ±30% with much of this error being dominated by the large differences between the Kochi and WHOI analyses. For Cl, the means of the EMP analyses and the three sets of Cs^+ primary beam SIMS analyses (WHOI, Nancy and Kochi) all agree, on average, within ±17%; the agreement is similar when the means are compared to the loaded amounts of Cl despite samples ND70-5-02 and ND70-6-02 being outside the calibration range for the SIMS analyses. The EMP, Nancy and Kochi SIMS analyses all agree on average within ±11%. In contrast, the agreement between the WHOI analyses and the other techniques is poorer (due to strong deviations on samples ND70-5-02 and ND70-6-02). For F, all three SIMS sessions (WHOI, Nancy, Kochi) agree with the loaded values, within ~14%, on average despite samples

520 ND70-5-02 and ND70-6-02 being outside the calibration range for all SIMS sessions. The
521 WHOI and Nancy SIMS sessions agree best, on average, within ±10%, while the Kochi
522 session agreement is poorer (due to strong deviations on samples ND70-5-02 and ND70-6-
523 02).

H_2O	ERDA	FTIR	SIMS Cs+ Caltech	SIMS Cs+ WHOI	SIMS O- WHOI	SIMS Cs+ Nancy	SIMS Cs+ Kochi	Average*
Loaded	6	6	11	8	9	7	14	9
ERDA		9	8	7	6	10	10	8
FTIR			12	13	10	10	19	11
SIMS Cs+ Caltech				12	10	11	15	11
SIMS Cs+ WHOI					12	9	13	11
SIMS O- WHOI						11	15	10
SIMS Cs+ Nancy							20	11
SIMS Cs+ Kochi								15

CO_2	NRA	EA	FTIR	SIMS Cs+ Caltech	SIMS O- Caltech	SIMS Cs+ WHOI	SIMS O- WHOI	SIMS Cs+ Nancy	SIMS Cs+ Kochi	EMPA	Average*
Loaded	101	9	69	48	59	140	155	115	64	85	85
NRA		8	13	42	25	32	24	47	23	12	33
EA			4	42	20	36	15	51	19	9	21
FTIR				28	15	22	14	38	14	19	23
SIMS Cs+ Caltech					33	17	35	14	37	74	37
SIMS O- Caltech						13	6	31	3	27	23
SIMS Cs+ WHOI							20	21	16	44	36
SIMS O- WHOI								30	8	31	34
SIMS Cs+ Nancy									48	97	49
SIMS Cs+ Kochi										23	25
EMPA											42

S	EMPA AMNH	SIMS Cs+ Caltech	SIMS Cs+ WHOI	SIMS Cs+ Nancy	SIMS Cs+ Kochi	Average*
Loaded	10	24	25	12	17	18
EMPA AMNH		16	15	15	29	17
SIMS Cs+ Caltech			13	30	54	27
SIMS Cs+ WHOI				38	140	46
SIMS Cs+ Nancy					12	21
SIMS Cs+ Kochi						50

Cl	Loaded	EMPA AMNH	SIMS Cs+ WHOI	SIMS Cs+ Nancy	SIMS Cs+ Kochi	Average*
Loaded		20	21	19	17	19
EMPA AMNH			21	10	11	16
SIMS Cs+ WHOI				24	16	21
SIMS Cs+ Nancy					13	16
SIMS Cs+ Kochi						14

F	Loaded	SIMS Cs+ WHOI	SIMS Cs+ Nancy	SIMS Cs+ Kochi	Average*
Loaded		15	12	15	14
SIMS Cs+ WHOI			5	33	18
SIMS Cs+ Nancy				30	16
SIMS Cs+ Kochi					26

*Average of mean absolute deviation across methods (in %)

524

***Figure 6**: Matrices showing the mean absolute deviation (in %) between all techniques used to measure H_2O, CO_2, S, Cl and F contents in the new reference materials. Background boxes colours are scaled with the mean absolute deviation from green to red. For each box, the mean absolute deviation is calculated by summing all absolute differences between the volatile contents determined by the row and column techniques normalized by the row technique and dividing by the number of analyses.*

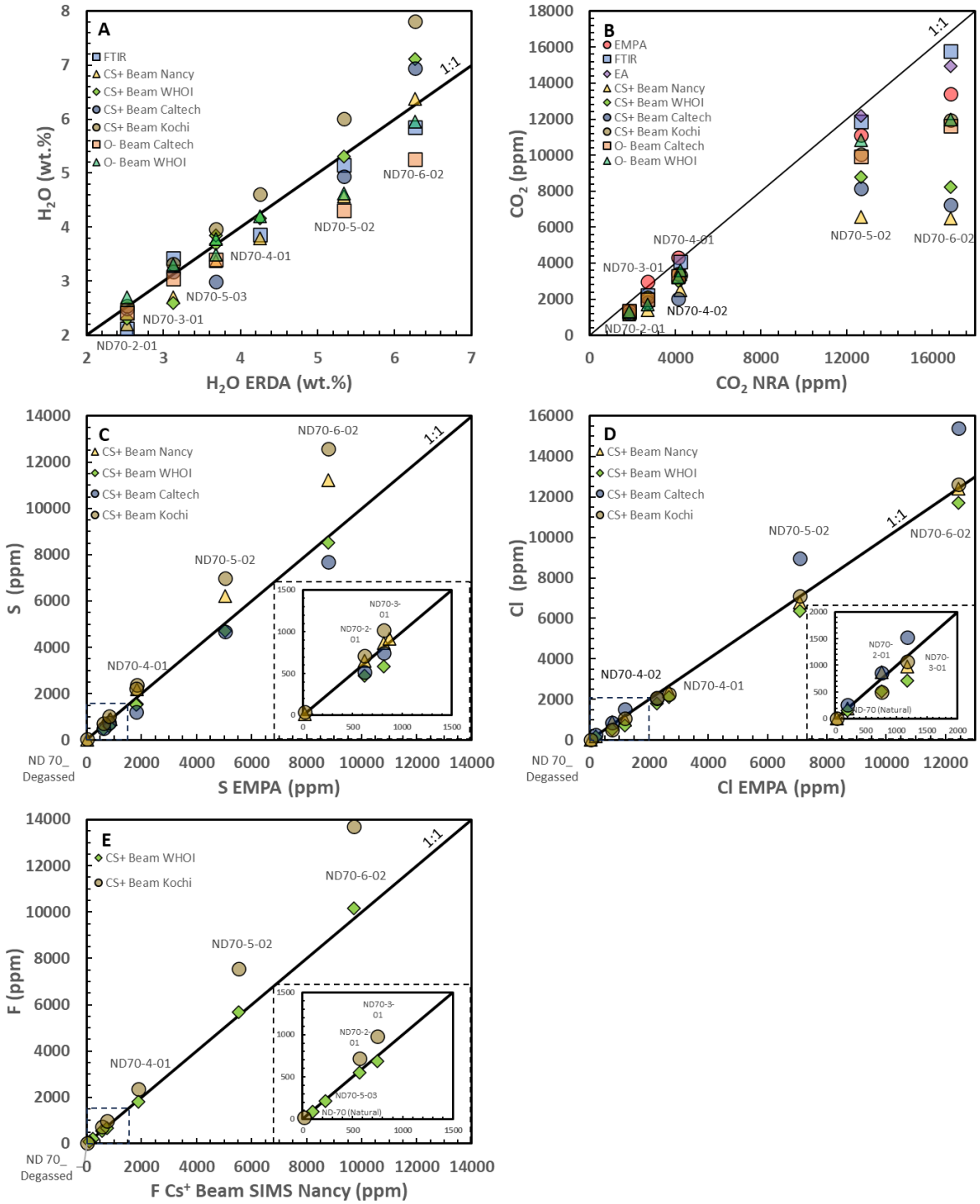

***Figure 7**: Comparison of measured H_2O, CO_2, S, Cl and F volatile content in ND70-series glasses by several techniques. With the exception of the last panel, the X-axis of each plot is the technique we have highest confidence in. All F analyses (panel E) were done by SIMS. Y-axis gives the value measured by all other techniques.*

b) Effect of water on SIMS CO_2 measurements

All four Cs^+ primary beam SIMS sessions (Kochi, Caltech, WHOI and Nancy), yielded CO_2 contents for ND70-6-02, that were low relative to the loaded abundance of CO_2. The loaded CO_2 abundance in sample ND70-6-02 was 1.5 wt.% (verified by FTIR, EA and NRA), yet the Cs^+ primary beam SIMS analyses at all four ion probes measured $^{12}C/^{30}Si$ ratios much lower than expected for such a mass fraction (see Fig. S3). In three out of four cases, the measured $^{12}C/^{30}Si$ ratios were even lower than those measured in sample ND70-5-02 which contained 1 wt.% CO_2. We attribute this anomaly to the high water mass fraction in the ND70-6-02 glass (> 6 wt%), limiting the ionization efficiency of ^{12}C, a phenomenon previously reported in an AGU abstract by Hervig et al. (2009) and similar to the decreasing yield of H^- ions observed with increasing water mass fraction (e.g., Hauri et al., 2002; Befus et al., 2020) although in this case the species are different.

Figure 8 shows the ionization efficiency ratios, $((^{12}C/^{30}Si)\times SiO_2)/CO_2$ and $(^{12}C/^{18}O)/CO_2$, as a function of the water content in all the glasses analysed during all SIMS sessions (note, we have not plotted glasses with CO_2 content near 0). If water had no effect on the ^{12}C ion probe signal, both ratios should remain constant as a function of water content. What we observe, however, is that these ratios vary greatly. At low water contents (<2 wt.%), the ratios are quite variable; in the Caltech and WHOI SIMS sessions, there is a hint of a possible positive correlation between C ionization efficiency and the glass water content, peaking at ~1.5 wt.% H_2O. At higher water contents (>2 wt.%), the C ionization efficiency seems to become more stable, at least in the explored range (2.5 to 6 wt.% H_2O), although there is still a hint of an inverse correlation between water content and C ionization efficiency (Fig. 8A and B). The fact that the C ionization efficiency is so variable between SIMS sessions suggests that the magnitude of the effect may be related to beam conditions.

Although Hervig et al. (2009) reported that using an O^- primary beam significantly mitigates the influence of H_2O on the carbon ion yield, we found that O^- primary beam analyses also suffered from the same effect (Fig. 8 C and D; note that the magnitude of the effect, although based on a smaller number of analyses, may potentially be less), The consequences of this C ionization efficiency reduction for SIMS carbon analyses are potentially dire. For example, if one were to analyse carbon in a natural basaltic glass containing 4 wt.% water using a Cs^+ primary beam and glass standards with less than 2 wt.% water, the unknown CO_2 mass

fractions could be underestimated by two to three-fold. The corollary is also true, using standards with high water contents to measure CO_2 mass fractions in samples with low water contents will result in large overestimations. It is likely that these effects permeate the literature of published glass and melt inclusion CO_2 concentration data. Thus, to accurately measure CO_2 by SIMS, one needs to select reference materials with water mass fractions matching that of the unknown sample or to characterise the signal dependency on water concentration as in Fig. 8.

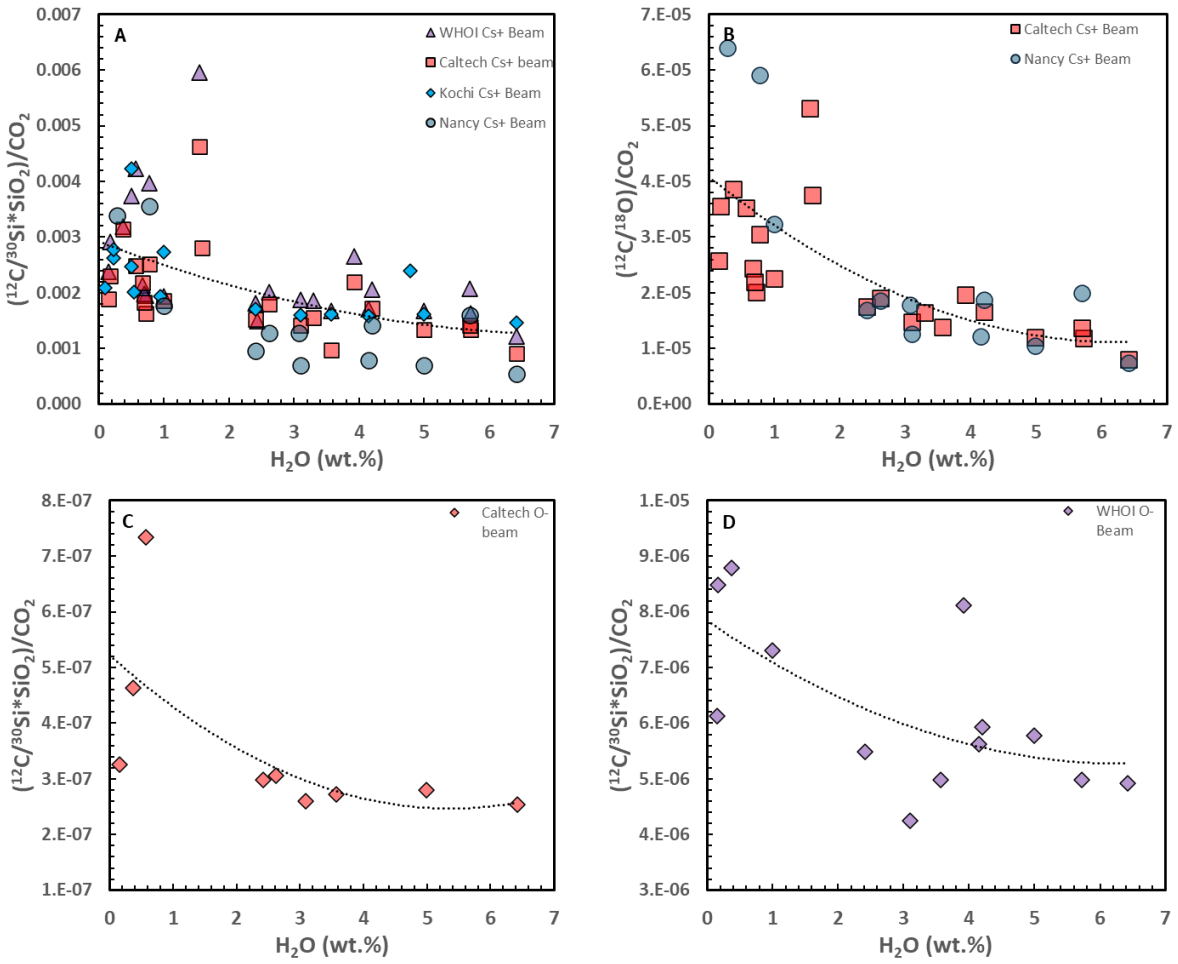

***Figure 8**: Effect of water on the $((^{12}C/^{30}Si)\times SiO_2)/CO_2$ and $(^{12}C/^{18}O)/CO_2$ ratios measured by SIMS (i.e., the calibration line). The results of four SIMS sessions using a Cs^+ primary beam and two SIMS sessions using a O^- primary beam are reported. In all cases the glass water content seems to greatly reduce the ionization efficiency of ^{12}C. Data used to generate the figure are reported in Table S9. Dotted lines are 2nd order polynomial best fit to all data.*

587 **c) Recommended values for ND70 glasses**

588 The compositions of the new reference materials we see as the most accurate, and which we
589 encourage researchers to use in future studies are reported in Table 6. For H_2O, since all
590 techniques agree within 13% (Fig. 6), we used the unweighted arithmetic mean values from
591 ERDA, FTIR, the three Cs^+ primary beam SIMS sessions at Caltech, WHOI and Nancy, the
592 O^- primary beam session at WHOI and the Cs^+ primary beam SIMS session at Kochi
593 (excluding samples ND70-5-02 and ND70-6-02 which were outside calibration range for the
594 Kochi session). We report the uncertainty as the standard deviation from these means. For
595 CO_2, given the strong effect of water on suppressing C ionization efficiency (see previous
596 section), we used the unweighted arithmetic mean of the NRA, EA and FTIR analyses and,
597 for the low C (<5000 ppm) samples, we also included the EMP analyses. We report the
598 uncertainty as the standard deviation from these means. For ND70_Natural we report the
599 unweighted arithmetic mean of all SIMS and FTIR sessions along with the associated
600 standard deviation. For S, since all techniques agreed reasonably well, we used the
601 unweighted arithmetic mean values from EMPA and the four Cs^+ primary beam SIMS
602 sessions (Caltech, WHOI, Kochi and Nancy) and report the uncertainty as the standard
603 deviation from these means. For Cl, we used the unweighted arithmetic mean values from
604 EMPA and three Cs^+ primary beam SIMS sessions at WHOI, Nancy and Kochi (but
605 excluding samples ND70-5-02 and ND70-6-02 from the WHOI session which deviated
606 significantly from all other estimates) and report the uncertainty as the standard deviation
607 from these means. For F, we used the mean values from three Cs^+ primary beam SIMS
608 sessions at WHOI, Nancy and Kochi (excluding samples ND70-5-02 and ND70-6-02 from
609 the Kochi session which deviated significantly from all other estimates) and report the
610 uncertainty as the standard deviation from these means.

611

612 **d) ND70 glasses, use and availability.**

613 The ND70 reference materials are now readily accessible to users at various Ion Microprobe
614 facilities, including those in France (CNRS-CRGP-Nancy and INSU-CNRS-IMPMC-Paris),
615 the United Kingdom (NERC-Edinburgh), Switzerland (SNF-Lausanne), the United States
616 (WHOI and Caltech), and Japan (JAMSTEC-Kochi). Furthermore, these resources are
617 available for researchers to borrow from the Smithsonian National Museum of Natural
618 History. Catalogue numbers for these materials are given in Table 6. We encourage
619 researchers to use at least a subset of these glasses (depending on the range of interest) to
620 improve the inter-comparability of future studies presenting microbeam analyses of H_2O,

CO_2, S, Cl and F in basaltic glasses. In particular, we expect the high volatile glasses to fill a gap in the standards currently available at most ion microprobe facilities.

VI. CONCLUSION

We present a new set of reference materials designed for *in situ* analysis of volatile elements (H_2O, CO_2, S, Cl, F) in basaltic silicate glass. The starting material was fused in air and 150 to 200mg splits with variable amounts of volatiles were subsequently run in the piston cylinder. The resulting reference glasses (the ND-70 series) span a wide range of mass fractions from 0 to 6 wt.% H_2O, 0 to 1.6 wt.% CO_2, and 0 to 1 wt.% S, Cl and F. The samples were characterized by Elastic Recoil Detection Analysis, Nuclear Reaction Analysis, Elemental Analyser, Fourier Transform Infrared Spectroscopy, Secondary Ion Mass Spectrometry, and Electron Microprobe.

Most analytical techniques provided good agreement with the expected volatile mass fractions in each of the glasses; agreement between techniques and between different ion probes is also generally good. CO_2 measurements are the exception and deviated significantly from expected values across analytical methods; however, inter-method reproducibility was good except for SIMS measurements. We found that this discrepancy in the SIMS results was likely due to the samples' high-water contents, which have a substantial impact on the ionization efficiency of ^{12}C during SIMS analyses. This underscores the importance of carefully selecting reference materials with water mass fractions matching those of unknown samples or characterizing the signal dependency on water content to ensure accurate CO_2 measurements by SIMS.

The reference materials we have presented in this study offer a community resource for the analysis of volatile elements in basaltic silicate glass, particularly when using SIMS and other micro-beam techniques. These materials are available to users at the Ion Microprobe facilities in France (CNRS-CRGP-Nancy and INSU-CNRS-IMPMC-Paris), the United Kingdom (NERC-Edinburgh), Switzerland (SNF-Lausanne), the United States (WHOI and Caltech) and Japan (JAMSTEC-Kochi). They are also freely available to researchers on a loan basis from the Smithsonian National Museum of Natural History (Catalogue numbers given in

Table 6). We encourage researchers to utilize them to improve the accuracy and inter-laboratory comparability of their measurements.

DATA AVAILABILITY STATEMENT

Raw FTIR spectra are archived as Moussallam (2024a). Raw NRA spectra are archived as Moussallam (2024b).

ACKNOWLEDGEMENTS

We thank Nordine Bouden and Johan Villeneuve for their invaluable support during the ion probe analyses at CNRS-CRPG-Nancy. We are very grateful to Richard Hervig and an anonymous reviewer for their comments which greatly improved the manuscript and to Thomas Meisel for editorial handling.

AUTHOR CONTRIBUTIONS

Initial study design: W.H.T., Y.M., T.P.

Experiments: W.H.T., Y.M., S.D.

ERDA: H.B., H.K.

NRA: H.B., H.K.

EA: H.L.

FTIR: S.D., H.L., S.S.

SIMS (Nancy): Y.M., E.R.K.

SIMS (WHOI): B.M., G.G.,

SIMS (Caltech): T.P., Y.G.

SIMS (Kochi): K.S., T.U.

EMPA (Caltech): E.M.S., M.B., C.M.

EMPA (AMNH): Y.M., S.D., W.H.T.

Visualisation and data compilation: Y.M.

Writing and interpretation: All authors, first draft Y.M.

REFERENCES

Albarède, F. (2009). Volatile accretion history of the terrestrial planets and dynamic implications. *Nature*, *461*(7268), 1227–1233. https://doi.org/10.1038/nature08477

683 Allard, P. (2010). A CO2-rich gas trigger of explosive paroxysms at Stromboli basaltic
684 volcano, Italy. *Journal of Volcanology and Geothermal Research*, *189*(3–4), 363–374.
685 https://doi.org/10.1016/j.jvolgeores.2009.11.018
686 Allison, C. M., Roggensack, K., & Clarke, A. B. (2019). H2O–CO2 solubility in alkali-rich
687 mafic magmas: new experiments at mid-crustal pressures. *Contributions to*
688 *Mineralogy and Petrology*, *174*(7), 58. https://doi.org/10.1007/s00410-019-1592-4
689 Armstrong, J. (1995). CITZAF: a package of correction programs for the quantitative
690 electron microbeam X-ray-analysis of thick polished materials, thin films, and
691 particles. *Microbeam Analysis*, *4*, 177.
692 Armstrong, J., & Crispin, K. (2013). Ultra-thin Iridium as a Replacement Coating for Carbon
693 in High Resolution Quantitative Analyses of Insulating Specimens. *Microscopy and*
694 *Microanalysis*, *19*(S2), 1070–1071. https://doi.org/10.1017/S1431927613007344
695 Befus, K. S., Walowski, K. J., Hervig, R. L., & Cullen, J. T. (2020). Hydrogen Isotope
696 Composition of a Large Silicic Magma Reservoir Preserved in Quartz-Hosted Glass
697 Inclusions of the Bishop Tuff Plinian Eruption. *Geochemistry, Geophysics,*
698 *Geosystems*, *21*(12), e2020GC009358. https://doi.org/10.1029/2020GC009358
699 Blank, Jennifer G., & Brooker, R. A. (1994). Experimental studies of carbon dioxide in
700 silicate melts; solubility, speciation, and sTable carbon isotope behavior. *Reviews in*
701 *Mineralogy and Geochemistry*, *30*(1), 157–186.
702 Blank, Jennifer Glee. (1993). *An experimental investigation of the behavior of carbon dioxide*
703 *in rhyolitic melt* (phd). California Institute of Technology.
704 https://doi.org/10.7907/tq3x-2059
705 Brooker, R., Holloway, J. R., & Hervig, R. (1998). Reduction in piston-cylinder experiments;
706 the detection of carbon infiltration into platinum capsules. *American Mineralogist*,
707 *83*(9–10), 985–994. https://doi.org/10.2138/am-1998-9-1006
708 Bureau, H., Raepsaet, C., Khodja, H., Carraro, A., & Aubaud, C. (2009). Determination of
709 hydrogen content in geological samples using elastic recoil detection analysis
710 (ERDA). *Geochimica et Cosmochimica Acta*, *73*(11), 3311–3322.
711 https://doi.org/10.1016/j.gca.2009.03.009
712 Caulfield, J., Turner, S., Arculus, R., Dale, C., Jenner, F., Pearce, J., et al. (2012). Mantle
713 flow, volatiles, slab-surface temperatures and melting dynamics in the north Tonga
714 arc–Lau back-arc basin. *Journal of Geophysical Research: Solid Earth*, *117*(B11).
715 https://doi.org/10.1029/2012JB009526

716 Clesi, V., Bouhifd, M. A., Bolfan-Casanova, N., Manthilake, G., Schiavi, F., Raepsaet, C., et
717 al. (2018). Low hydrogen contents in the cores of terrestrial planets. *Science*
718 *Advances*, *4*(3), e1701876. https://doi.org/10.1126/sciadv.1701876
719 Dasgupta, R., & Hirschmann, M. M. (2006). Melting in the Earth's deep upper mantle caused
720 by carbon dioxide. *Nature*, *440*(7084), 659–662. https://doi.org/10.1038/nature04612
721 Dehant, V., Debaille, V., Dobos, V., Gaillard, F., Gillmann, C., Goderis, S., et al. (2019).
722 Geoscience for Understanding Habitability in the Solar System and Beyond. *Space*
723 *Science Reviews*, *215*(6), 42. https://doi.org/10.1007/s11214-019-0608-8
724 Dixon, J. E., Stolper, E., & Delaney, J. R. (1988). Infrared spectroscopic measurements of
725 CO2 and H2O in Juan de Fuca Ridge basaltic glasses. *Earth and Planetary Science*
726 *Letters*, *90*(1), 87–104. https://doi.org/10.1016/0012-821X(88)90114-8
727 Edmonds, M., & Woods, A. W. (2018). Exsolved volatiles in magma reservoirs. *Journal of*
728 *Volcanology and Geothermal Research*, *368*, 13–30.
729 https://doi.org/10.1016/j.jvolgeores.2018.10.018
730 Eggler, D. H. (1976). Does CO2 cause partial melting in the low-velocity layer of the mantle?
731 *Geology*, *4*(2), 69–72. https://doi.org/10.1130/0091-
732 7613(1976)4<69:DCCPMI>2.0.CO;2
733 Ehlmann, B. L., Anderson, F. S., Andrews-Hanna, J., Catling, D. C., Christensen, P. R.,
734 Cohen, B. A., et al. (2016). The sustainability of habitability on terrestrial planets:
735 Insights, questions, and needed measurements from Mars for understanding the
736 evolution of Earth-like worlds. *Journal of Geophysical Research: Planets*, *121*(10),
737 1927–1961. https://doi.org/10.1002/2016JE005134
738 Elskens, I., Tazieff, H., & Tonani, F. (1968). Investigations Nouvelles sur les Gaz
739 Volcaniques. *Bulletin Volcanologique*, *32*(3), 521–574.
740 https://doi.org/10.1007/BF02599800
741 Foley, B. J., & Smye, A. J. (2018). Carbon Cycling and Habitability of Earth-Sized Stagnant
742 Lid Planets. *Astrobiology*, *18*(7), 873–896. https://doi.org/10.1089/ast.2017.1695
743 Hammerli, J., Hermann, J., Tollan, P., & Naab, F. (2021). Measuring in situ CO2 and H2O in
744 apatite via ATR-FTIR. *Contributions to Mineralogy and Petrology*, *176*(12), 105.
745 https://doi.org/10.1007/s00410-021-01858-6
746 Hauri, E., Wang, J., Dixon, J. E., King, P. L., Mandeville, C., & Newman, S. (2002). SIMS
747 analysis of volatiles in silicate glasses: 1. Calibration, matrix effects and comparisons
748 with FTIR. *Chemical Geology*, *183*(1–4), 99–114. https://doi.org/10.1016/S0009-
749 2541(01)00375-8

Hervig, R. L., Moore, G. M., & Roggensack, K. (2009). Calibrating Carbon Measurements in Basaltic Glass Using SIMS and FTIR: The Effect of Variable H2O Contents, *2009*, V51E-1755. Presented at the AGU Fall Meeting Abstracts.

Iacono-Marziano, G., Morizet, Y., Le Trong, E., & Gaillard, F. (2012). New experimental data and semi-empirical parameterization of H2O–CO2 solubility in mafic melts. *Geochimica et Cosmochimica Acta*, *97*, 1–23. https://doi.org/10.1016/j.gca.2012.08.035

Jarosewich, E., Nelen, J. a., & Norberg, J. A. (1980). Reference Samples for Electron Microprobe Analysis*. *Geostandards Newsletter*, *4*(1), 43–47. https://doi.org/10.1111/j.1751-908X.1980.tb00273.x

Jochum, K. P., Stoll, B., Herwig, K., Willbold, M., Hofmann, A. W., Amini, M., et al. (2006). MPI-DING reference glasses for in situ microanalysis: New reference values for element concentrations and isotope ratios. *Geochemistry, Geophysics, Geosystems*, *7*(2). https://doi.org/10.1029/2005GC001060

Joesten, R. L. (1974). *Metasomatism and magmatic assimilation at a gabbro-limestone contact, Christmas Mountains, Big Bend region, Texas* (phd). California Institute of Technology. Retrieved from https://resolver.caltech.edu/CaltechTHESIS:02272014-085454874

Kamenetsky, V. S., Everard, J. L., Crawford, A. J., Varne, R., Eggins, S. M., & Lanyon, R. (2000). Enriched End-member of Primitive MORB Melts: Petrology and Geochemistry of Glasses from Macquarie Island (SW Pacific). *Journal of Petrology*, *41*(3), 411–430. https://doi.org/10.1093/petrology/41.3.411

Keller, N. S., Arculus, R. J., Hermann, J., & Richards, S. (2008). Submarine back-arc lava with arc signature: Fonualei Spreading Center, northeast Lau Basin, Tonga. *Journal of Geophysical Research: Solid Earth*, *113*(B8). https://doi.org/10.1029/2007JB005451

Khodja, H., Berthoumieux, E., Daudin, L., & Gallien, J.-P. (2001). The Pierre Süe Laboratory nuclear microprobe as a multi-disciplinary analysis tool. *Nuclear Instruments and Methods in Physics Research Section B: Beam Interactions with Materials and Atoms*, *181*(1), 83–86. https://doi.org/10.1016/S0168-583X(01)00564-X

Krzhizhanovskaya, M. G., Chukanov, N. V., Mazur, A. S., Pautov, L. A., Varlamov, D. A., & Bocharov, V. N. (2023). Crystal chemistry and thermal behavior of B-, S- and Na-bearing spurrite. *Physics and Chemistry of Minerals*, *50*(4), 33. https://doi.org/10.1007/s00269-023-01257-2

Lesne, P., Scaillet, B., Pichavant, M., & Beny, J.-M. (2011). The carbon dioxide solubility in alkali basalts: an experimental study. *Contributions to Mineralogy and Petrology*, *162*(1), 153–168. https://doi.org/10.1007/s00410-010-0585-0

Lloyd, A. S., Plank, T., Ruprecht, P., Hauri, E. H., & Rose, W. (2013). Volatile loss from melt inclusions in pyroclasts of differing sizes. *Contributions to Mineralogy and Petrology*, *165*(1), 129–153. https://doi.org/10.1007/s00410-012-0800-2

Malavergne, V., Bureau, H., Raepsaet, C., Gaillard, F., Poncet, M., Surblé, S., et al. (2019). Experimental constraints on the fate of H and C during planetary core-mantle differentiation. Implications for the Earth. *Icarus*, *321*, 473–485. https://doi.org/10.1016/j.icarus.2018.11.027

Mayer, M. (1999). SIMNRA, a simulation program for the analysis of NRA, RBS and ERDA. *AIP Conference Proceedings*, *475*(1), 541–544. https://doi.org/10.1063/1.59188

Métrich, N., & Wallace, P. J. (2008). Volatile Abundances in Basaltic Magmas and Their Degassing Paths Tracked by Melt Inclusions. *Reviews in Mineralogy and Geochemistry*, *69*(1), 363–402. https://doi.org/10.2138/rmg.2008.69.10

Mosbah, M., Metrich, N., & Massiot, P. (1991). PIGME fluorine determination using a nuclear microprobe with application to glass inclusions. *Nuclear Instruments and Methods in Physics Research Section B: Beam Interactions with Materials and Atoms*, *58*(2), 227–231. https://doi.org/10.1016/0168-583X(91)95592-2

Moussallam, Y. (2024a). ND70 paper_Raw FTIR spectra [Data set]. figshare. https://doi.org/10.6084/m9.figshare.25292692.v1

Moussallam, Y. (2024b). ND70 paper_Raw NRA Spectra [Data set]. figshare. https://doi.org/10.6084/m9.figshare.25292674.v1

Moussallam, Y., Morizet, Y., Massuyeau, M., Laumonier, M., & Gaillard, F. (2015). CO2 solubility in kimberlite melts. *Chemical Geology*, *418*, 198–205. https://doi.org/10.1016/j.chemgeo.2014.11.017

Moussallam, Y., Oppenheimer, C., Scaillet, B., Buisman, I., Kimball, C., Dunbar, N., et al. (2015). Megacrystals track magma convection between reservoir and surface. *Earth and Planetary Science Letters*, *413*, 1–12. https://doi.org/10.1016/j.epsl.2014.12.022

Moussallam, Y., Morizet, Y., & Gaillard, F. (2016). H2O–CO2 solubility in low SiO2-melts and the unique mode of kimberlite degassing and emplacement. *Earth and Planetary Science Letters*, *447*, 151–160. https://doi.org/10.1016/j.epsl.2016.04.037

816 Moussallam, Y., Lee, H. J., Ding, S., DeLessio, M., Everard, J. L., Spittle, E., et al. (2023).
817 Temperature of the Villarrica Lava Lake from 1963 to 2015 Constrained by Phase-
818 Equilibrium and a New Glass Geothermometer for Basaltic Andesites. *Journal of*
819 *Petrology*, *64*(2). https://doi.org/10.1093/petrology/egad003
820 Nicoli, G., & Ferrero, S. (2021). Nanorocks, volatiles and plate tectonics. *Geoscience*
821 *Frontiers*, *12*(5), 101188. https://doi.org/10.1016/j.gsf.2021.101188
822 Shi, S. C., Towbin, W. H., Plank, T., Barth, A., Rasmussen, D., Moussallam, Y., et al.
823 (2023). PyIRoGlass: An Open-Source, Bayesian MCMC Algorithm for Fitting
824 Baselines to FTIR Spectra of Basaltic-Andesitic Glasses. Retrieved from
825 https://eartharxiv.org/repository/view/6193/
826 Shimizu, Kei, Saal, A. E., Hauri, E. H., Perfit, M. R., & Hékinian, R. (2019). Evaluating the
827 roles of melt-rock interaction and partial degassing on the CO2/Ba ratios of MORB:
828 Implications for the CO2 budget in the Earth's depleted upper mantle. *Geochimica et*
829 *Cosmochimica Acta*, *260*, 29–48. https://doi.org/10.1016/j.gca.2019.06.013
830 Shimizu, Kenji, Suzuki, K., Saitoh, M., Konno, U., Kawagucci, S., & Ueno, Y. (2015).
831 Simultaneous determinations of fluorine, chlorine, and sulfur in rock samples by ion
832 chromatography combined with pyrohydrolysis. *Geochemical Journal*, *49*(1), 113–
833 124. https://doi.org/10.2343/geochemj.2.0338
834 Shimizu, Kenji, Ushikubo, T., Hamada, M., Itoh, S., Higashi, Y., Takahashi, E., & Ito, M.
835 (2017). H_2O, CO_2, F, S, Cl, and P_2O_5 analyses of silicate glasses using SIMS: Report
836 of volatile standard glasses. *Geochemical Journal*, *51*(4), 299–313.
837 https://doi.org/10.2343/geochemj.2.0470
838 Shishkina, T. A., Botcharnikov, R. E., Holtz, F., Almeev, R. R., & Portnyagin, M. V. (2010).
839 Solubility of H2O- and CO2-bearing fluids in tholeiitic basalts at pressures up to
840 500 MPa. *Chemical Geology*, *277*(1–2), 115–125.
841 https://doi.org/10.1016/j.chemgeo.2010.07.014
842 Stern, R. J. (2018). The evolution of plate tectonics. *Philosophical Transactions of the Royal*
843 *Society A: Mathematical, Physical and Engineering Sciences*, *376*(2132), 20170406.
844 https://doi.org/10.1098/rsta.2017.0406
845 Stolper, E., & Holloway, J. R. (1988). Experimental determination of the solubility of carbon
846 dioxide in molten basalt at low pressure. *Earth and Planetary Science Letters*, *87*(4),
847 397–408. https://doi.org/10.1016/0012-821X(88)90004-0

Tamic, N., Behrens, H., & Holtz, F. (2001). The solubility of H2O and CO2 in rhyolitic melts in equilibrium with a mixed CO2-H2O fluid phase. *Chemical Geology*, *174*(1–3), 333–347. https://doi.org/10.1016/S0009-2541(00)00324-7

Webster, J. D., Goldoff, B., & Shimizu, N. (2011). C–O–H–S fluids and granitic magma: how S partitions and modifies CO2 concentrations of fluid-saturated felsic melt at 200 MPa. *Contributions to Mineralogy and Petrology*, *162*(4), 849–865. https://doi.org/10.1007/s00410-011-0628-1

Wyllie, P. J. (1971). Role of water in magma generation and initiation of diapiric uprise in the mantle. *Journal of Geophysical Research (1896-1977)*, *76*(5), 1328–1338. https://doi.org/10.1029/JB076i005p01328

TABLES

Table 1. Expected chemical composition (in wt.% unless otherwise indicated) of all experiments based on loaded amounts of starting material.

Sample Name	SiO_2	TiO_2	Al_2O_3	FeO_{tot}	MnO	MgO	CaO	Na_2O	K_2O	P_2O_5	H_2O	CO_2 (ppm)	S (ppm)	Cl (ppm)	F (ppm)	Total
ND 70_ Degassed	50.18	0.85	16.54	8.18	0.17	8.44	13.18	2.21	0.17	0.09	0.00	0	0	0	0	100
ND70-2-01	48.74	0.82	16.06	7.95	0.17	8.28	13.01	2.20	0.17	0.08	2.25	665	672	679	717	100
ND70-3-01	48.15	0.81	15.87	7.85	0.16	8.21	12.95	2.21	0.16	0.08	3.13	989	1001	1011	1067	100
ND70-4-01	47.26	0.80	15.58	7.71	0.16	8.18	13.01	2.26	0.16	0.08	3.99	1970	1993	2013	2125	100
ND70-4-02	47.15	0.80	15.54	7.69	0.16	8.16	12.98	2.25	0.16	0.08	4.22	1965	1988	2008	2120	100
ND70-5-02	47.27	0.71	13.88	6.87	0.14	7.67	13.27	2.33	0.14	0.07	5.01	10349	5072	5468	5497	100
ND70-5-03	48.17	0.81	15.88	7.85	0.16	8.13	12.71	2.14	0.16	0.08	3.82	197	200	202	213	100
ND70-6-02	44.29	0.67	13.01	6.43	0.13	7.71	14.06	2.64	0.13	0.07	6.28	15023	10177	10363	10112	100

Table 2. Experimental conditions.

Experiment #	Pressure (MPa)	Temperature (°C)	Duration (h)
ND 70_ Degassed	0.1	1350	4
ND70-2-01	1000	1325	2
ND70-3-01	1000	1325	2
ND70-4-01	1000	1225	2
ND70-4-02	1000	1325	2
ND70-5-02	1500	1325	2
ND70-5-03	1500	1325	2
ND70-6-02	1500	1325	2

867 **Table 3**. Measured major and volatile composition by electron microprobe (in wt.% unless
868 otherwise indicated) of experimental glasses and other glasses analysed during the same
869 analytical sessions. n denotes the number of analyses from which averages are reported.
870 Errors (two standard deviation) are ±0.43 for SiO_2, ±0.18 for Na_2O, ±0.02 for K_2O, ±0.17 for
871 Al_2O_3, ±0.36 for CaO, ±0.24 for FeO, ±0.11 for MgO, ±0.04 for TiO_2, ±0.05 for MnO, ±0.04
872 for P_2O_5, ±0.01 for S and ±0.03 for Cl.

	EMPA (AMNH)										
Experiment #	n	SiO_2	TiO_2	Al_2O_3	FeO_{tot}	MnO	MgO	CaO	Na_2O	K_2O	P_2O_5	S (ppm)
ND 70_ Degassed	5	49.68	0.80	16.12	8.27	0.14	8.71	13.01	2.22	0.16	0.09	15
ND70-2-01	10	47.81	0.76	15.58	8.00	0.15	8.51	12.66	2.17	0.17	0.08	621
ND70-3-01	10	47.18	0.77	15.21	8.04	0.15	8.61	12.76	2.09	0.16	0.08	814
ND70-4-01	10	47.37	0.75	15.13	7.60	0.16	8.23	12.30	2.19	0.16	0.07	1831
ND70-4-02	10	44.27	0.73	14.54	7.59	0.14	8.23	12.60	2.21	0.16	0.09	1796
ND70-5-02	10	46.12	0.65	13.21	6.83	0.12	7.89	13.15	2.34	0.15	0.07	5045
ND70-6-02	12	44.01	0.64	12.62	6.19	0.11	8.22	13.16	2.12	0.18	0.08	8786
Other glasses analysed												
ND-70 (Natural)	3	49.92	0.81	16.11	8.17	0.15	8.27	12.95	2.10	0.16	0.09	871
VILLA_P2	12	50.60	1.29	15.42	9.15	0.16	5.41	8.55	3.10	0.75	0.28	3529
INSOL_MX1_BA4	1	52.36	1.62	12.87	8.12	0.11	9.55	10.53	2.66	1.41	0.23	18

873

874

875

876 **Table 4**. ERDA, NRA, EA and FTIR measurements (in wt.% for H_2O and in ppm for all
877 other species) of experimental glasses and other glasses analysed during the same analytical
878 sessions. All errors are given as one standard deviation on repeat analyses or as one standard
879 deviation from analytical error (whichever is the highest), n denotes the number of analyses
880 from which averages are reported.

	ERDA (CEA-CNRS-Saclay)			NRA (CEA-CNRS-Saclay)			EA (LDEO)			FTIR (LDEO)				EMPA (Caltech)		
Experiment #	n	H_2O	±	n	CO_2	±	n	CO_2	±	n	H_2O	±	CO_2	±	n	CO_2 (ppm)	±
ND 70_ Degassed																	
ND70-2-01	2	2.53	0.24	1	1837	35				6	2.12	0.34	1283	120			
ND70-3-01	2	3.13	0.30	1	2689	54				7	3.43	0.97	2226	403	5	2997	365
ND70-4-01	1	4.25	0.40	1	4228	71				8	3.86	0.89	4095	621			
ND70-4-02	2	3.68	0.35	1	4122	65									5	4306	794
ND70-5-02	2	5.34	0.51	1	12682	105	1	12160	891	6	5.15	0.59	11868	1204	5	11125	1876
ND70-5-03	1	3.68	0.35														
ND70-6-02	2	6.26	0.59	1	16847	120	1	14940	1095	3	5.85	0.96	15754	1835	5	13397	313
Other glasses analysed																	
ND-70 (Natural)										3	0.66	0.15	59	23			
Suprasil	2	0.02	0.00														
BF73	2	0.73	0.07	1	2832	56				3	0.82	0.06	3042	84	5	6579	3594
BF76										3	0.75	0.06	2319	68	5	3560	266
BF77										3	0.86	0.08	891	47	5	2506	145
M15																	
M19															5	5198	1720
M20	1	5.82	0.55	1	2417	51									5	3056	1160
M34																	
M35	1	4.31	0.41	1	1436	40				3	4.1	0.45	1000	75	5	3119	3414
M40																	
M43										3	2.52	0.25	2857	154	5	3300	536
M48																	
KL2																	
KE12																	
40428																	
47963																	
N72																	
ALV519-4-1																	
ALV1846-12																	
80-1-3																	
ALV1846-9										3	1.	0.	18	8			

NS-1					3	43 0. 35	12 0. 03	354 6	12 9	5	4708	10 60
Villa_P2					6	3. 92	0. 7	835	74			
INSOL_MX1_BA4					3	0. 15	0. 01	820 7	37 7			
VG2												

881
882
883
884
885

Table 5. SIMS measurements (in wt.% for H_2O and in ppm for all other species) of experimental glasses and other glasses analysed during the same analytical sessions. Errors are calculated using two standard error (i.e., 95% confidence interval) on calibration lines for each session, n denotes the number of analyses from which averages are reported. Values in red were determined outside calibration range.

	SIMS (CNRS-Nancy, Cs+beam)										
Experiment #	n	H_2O	±	CO_2	±	S	±	Cl	±	F	±
ND 70_ Degassed	2	0.03	0.00	66	6	17	1	4	0	13	1
ND70-2-01	3	2.21	0.06	1141	101	649	42	876	110	572	40
ND70-3-01	2	2.70	0.07	1397	124	862	56	983	124	745	52
ND70-4-01	2	3.79	0.10	2519	224	*2207*	*142*	2401	302	1896	133
ND70-5-02	2	4.57	0.12	*6566*	*583*	*6211*	*400*	*6777*	*852*	*5538*	*388*
ND70-5-03	2	3.37	0.09	1098	98	175	11	326	41	228	16
ND70-6-02	2	6.37	0.17	*6482*	*576*	*11214*	*722*	*12405*	*1559*	*9725*	*681*
Other glasses analysed											
ND-70 (Natural)	1	1.04	0.03	195	17	916	59	194	24	98	7
M34	3	5.59	0.15	458	41	11	1	36	4	79	6
M35	10	4.14	0.11	1100	98	11	1	33	4	75	5
M40	10	3.31	0.09	2118	188	12	1	33	4	73	5
M43	1	2.70	0.07	3071	273	5	0	29	4	68	5
M48	10	0.82	0.02	477	42	3	0	28	4	64	4
KL2	10	0.01	0.00	157	14	6	0	14	2	58	4
KE12	10	0.16	0.00	116	10	264	17	3419	430	4251	298
40428	9	0.88	0.02	256	23	889	57	349	44	413	29
47963	10	1.23	0.03	229	20	646	42	902	113	638	45
N72	5	0.02	0.00	186	17	4	0	28	4	77	5
VG2	10	0.34	0.01	396	35	1450	93	233	29	160	11
	SIMS (WHOI, Cs+beam)										
Experiment #	n	H_2O	±	CO_2	±	S	±	Cl	±	F	±

ND70-2-01	3	2.31	0.10	1204	92	476	57	518	14	550	47
ND70-3-01	2	2.59	0.12	2106	160	582	70	708	20	683	58
ND70-4-01	3	4.16	0.19	3037	231	1553	187	2125	59	1808	155
ND70-4-02	3	3.69	0.17	3026	231	1505	181	1811	50	1665	142
ND70-5-02	3	5.31	0.24	8770	668	*4714*	*567*	*6357*	*177*	*5694*	*487*
ND70-5-03	3	3.85	0.17	1412	108	128	15	300	8	217	19
ND70-6-02	3	7.11	0.32	8216	626	*8525*	*1026*	*11713*	*326*	*10177*	*870*
Other glasses analysed											
ND-70 (Natural)	3	1.02	0.05	120	9	625	75	160	4	86	7
Suprasil	3	0.01	0.00	25	2	0	0	1912	53	3	0
BF73	2	0.87	0.04	2502	191	0	0	36	1	36	3
BF76	2	0.82	0.04	2134	163	0	0	34	1	27	2
BF77	3	0.82	0.04	791	60	0	0	34	1	27	2
M15	3	1.64	0.07	152	12	1	0	21	1	53	5
M19	3	3.06	0.14	2608	199	3	0	21	1	54	5
M20	3	5.76	0.26	1689	129	8	1	25	1	62	5
M34	3	5.52	0.25	332	25	6	1	24	1	60	5
M35	3	4.41	0.20	896	68	5	1	24	1	60	5
M43	3	2.76	0.13	2720	207	2	0	23	1	55	5
M48	3	0.76	0.03	298	23	0	0	19	1	50	4
KE12	3	0.20	0.01	5	0	204	25	3287	92	4220	361
ALV519-4-1	5	0.19	0.01	205	16	614	74	39	1	62	5
80-1-3	3	0.64	0.03	532	41	596	72	47	1	161	14
1846-9	4	1.78	0.08	9	1	236	28	206	6	269	23
NS-1	3	0.42	0.02	4295	327	31	4	24	1	60	5
Villa_P2	3	4.67	0.21	946	72	3638	438	106	3	144	12
INSOL_MX1_BA4	3	0.22	0.01	8314	634	8	1	81	2	271	23

Run101@2.asc	3	1.93	0.09	55	4	285	34	570	16	268	23
Run10@2.asc	3	4.35	0.20	23	2	20	2	401	11	4	0
ALV_1833-1	3	2.28	0.10	15	1	497	60	553	15	254	22
WOK28-3	3	0.52	0.02	292	22	650	78	45	1	95	8
	SIMS (Caltech, Cs+beam)										
Experiment #	n	H_2O	±	CO_2	±	S	±	Cl	±	F	±
ND70-2-01	2	2.49	0.09	1183	117	513	84	*859*	*156*	*1247*	*99*
ND70-3-01	8	3.18	0.12	1851	184	745	122	*1527*	*277*	*1828*	*145*
ND70-4-02	3	2.99	0.11	2039	202	1219	199	*2061*	*374*	*2658*	*210*
ND70-5-02	2	4.94	0.18	8151	808	*4687*	*766*	*8955*	*1626*	*12118*	*959*
ND70-6-02	2	6.95	0.26	7234	718	*7687*	*1257*	*15406*	*2798*	*20358*	*1611*
Other glasses analysed											
ND-70 (Natural)	2	1.09	0.04	135	13	657	107	257	47	193	15
Suprasil	2	0.00	0.00	2	0	0	0	*2456*	*446*	0	0
BF73	2	0.79	0.03	2435	242	0	0	53	10	73	6
BF76	2	0.85	0.03	2534	251	0	0	54	10	61	5
BF77	2	0.83	0.03	853	85	0	0	51	9	57	5
M15	2	1.68	0.06	138	14	1	0	32	6	115	9
M19	2	3.41	0.13	2520	250	3	1	35	6	122	10
M20	2	5.36	0.20	1609	160	8	1	39	7	132	10
M34	1	5.40	0.20	265	26	6	1	34	6	124	10
M35	2	4.15	0.15	869	86	5	1	34	6	126	10
M43	1	2.80	0.10	2834	281	2	0	35	6	121	10
M48	1	0.84	0.03	221	22	0	0	31	6	113	9
ALV519-4-1	2	0.16	0.01	189	19	541	88	46	8	111	9
1846-12	2	1.38	0.05	126	12	617	101	347	63	282	22
80-1-3	2	0.55	0.02	365	36	566	93	60	11	317	25
1846-9	2	1.7	0.0	7	1	223	36	275	50	574	45

NS-1	3	1 0.42	6 0.02	4931	489	32	5	36	6	135	11
Villa_P2	2	4.52	0.17	909	90	3698	604	151	27	303	24
INSOL_MX1_BA4	2	0.18	0.01	7737	767	6	1	95	17	492	39
Run101@2.asc	2	1.74	0.06	49	5	252	41	781	142	548	43
Run10@2.asc	2	3.78	0.14	14	1	16	3	482	88	2	0
	SIMS (JAMSTEC-Kochi) Cs+ primary beam										
Experiment #	n	H2O	±	CO2	±	S	±	Cl	±	F	±
ND 70_ Degassed	2	0.03	0.00	8	0	39	1	12	1	16	1
ND70-2-01	3	2.55	0.09	1339	61	709	24	495	44	722	39
ND70-3-01	3	3.32	0.11	2121	96	1017	34	1068	96	982	53
ND70-4-01	3	4.62	0.16	3320	151	*2365*	*80*	2276	204	2355	126
ND70-4-02	3	3.96	0.14	3421	155	*2238*	*76*	2101	188	2109	113
ND70-5-02	3	*6.00*	*0.21*	*10034*	*455*	*6982*	*236*	*7095*	*636*	*7543*	*404*
ND70-6-02	3	*7.81*	*0.27*	*11934*	*542*	*12567*	*426*	*12606*	*1130*	*13703*	*735*
Other glasses (and minerals) analyzed											
ND-70 (Natural)	2	1.06	0.04	200	9	883	30	176	16	105	6
Vol-std-G_EPR-G3	5	0.24	0.01	355	16	1236	42	118	11	117	6
Vol-std-G_SC-ol	1	0.00	0.00	9	0	0	0	0	0	1	0
Vol-std-G_ELA-qz	4	0.01	0.00	12	1	0	0	0	0	1	0
Vol-std-G_IND-G1	1	0.51	0.02	206	9	1043	35	78	7	172	9
Vol-std-G_Vol-3A	1	3.46	0.12	4786	217	1046	35	2547	228	2996	161
Vol-std-G_Vol-1B	1	0.94	0.03	4546	206	673	23	743	67	847	45
Vol-std-G_Vol-05A	1	0.57	0.02	3384	154	521	18	272	24	418	22
Vol-std-G_Vol-005B	1	0.09	0.00	503	23	44	1	32	3	46	2
Vol-std-G_MRN-G1	1	2.12	0.07	6	0	72	2	2854	256	650	35
Vol-std-G_MA42	1	4.74	0.16	1492	68	29	1	111	10	72	4
Vol-std-G_FJ-G2	1	0.2	0.0	429	19	1328	45	90	8	117	6

Vol-std-G_IND-G2	4	1									
	1	0.54	0.02	482	22	1042	35	80	7	209	11
Vol-std-G_vol-0B	1	0.02	0.00	8	0	1	0	1	0	5	0

	SIMS (WHOI, O-beam)				
Experiment #	n	H_2O	±	CO_2	±
ND70-2-01	3	2.70	0.11	1315	148
ND70-3-01	5	3.31	0.14	1721	193
ND70-4-01	5	4.21	0.18	3595	404
ND70-4-02	3	3.49	0.15	3219	362
ND70-5-02	3	4.62	0.19	*10855*	*1220*
ND70-5-03	3	3.79	0.16	1655	186
ND70-6-02	3	5.96	0.25	*11981*	*1346*
Other glasses analyzed					
ND-70 (Natural)	3	1.12	0.05	163	18
Suprasil	3	0.01	0.00	30	3
M20	3	5.49	0.23	1851	208
M35	3	4.10	0.17	927	104
ALV519-4-1	3	0.20	0.01	215	24
NS-1	3	0.48	0.02	4254	478
Villa_P2	3	4.26	0.18	1040	117
INSOL_MX1_BA4	3	0.24	0.01	7718	867

	SIMS (Caltech, O-beam)				
Experiment #	n	H_2O	±	CO_2	±
ND70-2-01	2	2.42	0.15	1343	184
ND70-3-01	*8*	*3.05*	*0.19*	1979	271
ND70-4-02	*3*	*3.40*	*0.21*	3309	454
ND70-5-02	*2*	*4.31*	*0.26*	*9928*	*1361*

ND70-6-02	*2*	*5.26*	*0.32*	*11615*	*1593*
Other glasses analyzed ND-70 (Natural)					
Suprasil	1	0.00	0.00	0	0
M43	1	2.58	0.16	2806	385
80-1-3	2	0.68	0.04	626	86
NS-1	3	0.45	0.03	4223	579
INSOL_MX1_BA4	2	0.23	0.01	7729	1060

Table 6. Major element and volatile content of the new reference glasses. For H_2O we used the mean values from ERDA, FTIR, the three Cs^+ primary beam SIMS sessions at Caltech, WHOI and Nancy, the O^- primary beam session at WHOI and the Cs^+ primary beam SIMS sessions at Kochi but excluding samples ND70-5-02 and ND70-6-02, outside calibration range in that session. We report the uncertainty as the standard deviation from these means. For CO_2 we used the mean of the NRA, EA and FTIR analyses and, for the low C (<5000 ppm) samples, we also included the EMP analyses. We report the uncertainty as the standard deviation from these means. For ND70_Natural we report the mean of all SIMS and FTIR sessions along with the associated standard deviation. For S, we used the mean values from EMPA and the four Cs^+ primary beam SIMS sessions (Caltech, WHOI, Kochi and Nancy) and report the uncertainty as the standard deviation from these means. For Cl, we used the mean values from EMPA and three Cs^+ primary beam SIMS sessions at WHOI, Nancy and Kochi (but excluding samples ND70-5-02 and ND70-6-02 from the WHOI session which deviated significantly from all other estimates) and report the uncertainty as the standard deviation from these means. For F, we used the mean values from three Cs^+ primary beam SIMS sessions at WHOI, Nancy and Kochi (but excluding samples ND70-5-02 and ND70-6-02 from the Kochi session which deviated significantly from all other estimates) and report the uncertainty as the standard deviation from these means. International Generic Sample Number (IGSN) and catalogue numbers from the Smithsonian National Museum of Natural History (NMNH) Rock & Ore Collections are provided.

Sample #	IGSN:	NMNH catalogue number	Majors (normalized)											Volatiles									
			SiO_2	TiO_2	Al_2O_3	FeO_{tot}	MnO	MgO	CaO	Na_2O	K_2O	P_2O_5	sum	H_2O	±	CO_2 (ppm)	±	S (ppm)	±	Cl (ppm)	±	F (ppm)	±
ND 70_ Degassed	10.58052/IEYM10001	118554-1	50.09	0.80	16.25	8.34	0.14	8.78	13.11	2.23	0.16	0.09	100	blank		blank		24	13	11	8	15	2
ND-70 (Natural)		118554-8	50.56	0.82	16.32	8.27	0.15	8.38	13.12	2.13	0.16	0.09	100	1.00	0.17	145	53	790	138	182	18	96	9
ND70-2-01	10.58052/IEYM10002	118554-2	49.86	0.79	16.25	8.34	0.16	8.87	13.20	2.26	0.17	0.08	100	2.41	0.21	1560	392	594	97	661	185	615	93
ND70-3-01	10.58052/IEYM10003	118554-3	49.64	0.81	16.00	8.46	0.15	9.06	13.42	2.20	0.17	0.08	100	3.09	0.32	2637	388	804	160	984	200	803	158
ND70-4-01	10.58052/IEYM10004	118554-4	50.43	0.80	16.10	8.09	0.17	8.76	13.09	2.33	0.17	0.07	100	4.15	0.30	4161	94	1989	367	2368	231	2020	294

ND70-4-02	10.58052/IEYM10005	118554-5	48.88	0.80	16.05	8.39	0.16	9.09	13.92	2.43	0.18	0.10	100	3.56	0.36	4214	1309	1689	435	2060	2321	1887	3144	
ND70-5-02	10.58052/IEYM10006	118554-6	50.94	0.72	14.59	7.55	0.13	8.72	14.52	2.58	0.16	0.08	100	4.99	0.34	12237	4128	5528	1023	6984	1180	5616	1110	
ND70-6-02	10.58052/IEYM10007	118554-7	50.39	0.73	14.45	7.09	0.13	9.41	15.06	2.43	0.21	0.09	100	6.42	0.51	15847	9576	9756	2047	12293	3961	9951	3199	

SUPPLEMENTARY to: "ND70-series basaltic glass reference materials for volatile element (H_2O, CO_2, S, Cl, F) analyses and the C ionization efficiency supressing effect of water in silicate glasses."

Yves Moussallam[1], William Henry Towbin[2], Terry Plank[1], Hélène Bureau[3], Hicham Khodja[4], Yunbin Guan[5], Chi Ma[5], Michael B. Baker[5], Edward M. Stolper[5], Fabian U. Naab[6], Brian D. Monteleone[7], Glenn G. Gaetani[7], Kenji Shimizu[8], Takayuki Ushikubo[8], Hyun Joo Lee[1], Shuo Ding[1], Sarah Shi[1], Estelle F. Rose-Koga[9].

[1] *Lamont-Doherty Earth Observatory, Columbia University, New York, USA*

[2] *Gemological Institute of America, 50 W. 47th Street, New York, NY 10036, United States of America*

[3] *IMPMC, Sorbonne Université, CNRS UMR 7590, MNHN, IRD UR 206, 4 place Jussieu, 75252 Paris Cedex 05, France*

[4] *LEEL, NIMBE, CEA, CNRS, Université Paris−Saclay, CEA Saclay, 91191 Gif sur Yvette Cedex, France*

[5] *Division of Geological and Planetary Sciences, California Institute of Technology, Pasadena, California 91125, USA*

[6] *Department of Nuclear Engineering and Radiological Sciences, University of Michigan, Ann Arbor, Michigan 48109, USA*

[7] *Department of Geology and Geophysics, Woods Hole Oceanographic Institution, Woods Hole, MA 02543, USA.*

[8] *Kochi Institute for Core Sample Research, Japan Agency for Marine-Earth Science and Technology, Monobe-otsu 200, Nankoku, Kochi 783-8502, Japan*

[9] *ISTO, UMR 7327, CNRS-UO-BRGM, 1A rue de la Férollerie, 45071 Orléans cedex 2, France*

Corresponding author: Yves Moussallam; yves.moussallam@ldeo.columbia.edu

SUPPLEMENTARY FIGURES

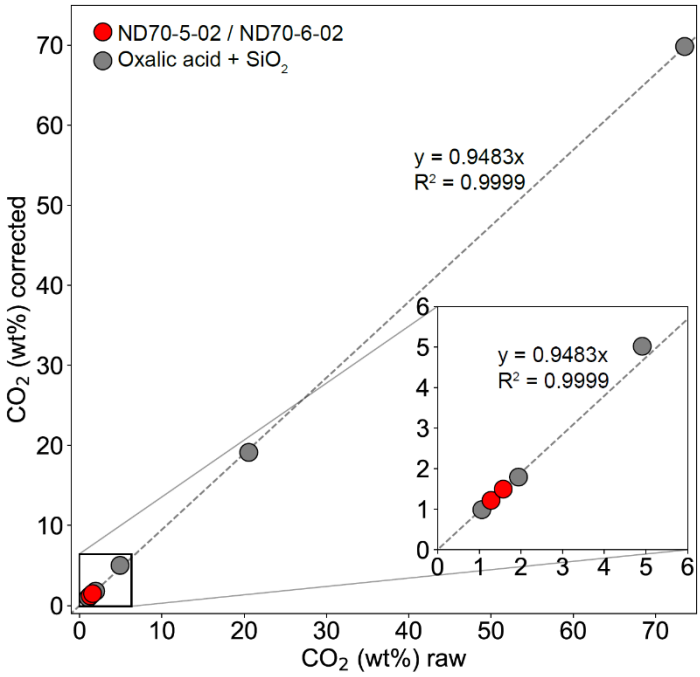

***Figure S1**: Elemental Analyser secondary calibration. CO_2 (wt%) raw indicates the raw EA result calibrated by acetanilide. CO_2 (wt%) corrected is calibrated by a series of oxalic acid and SiO_2 mixtures. Gray circles are oxalic acid and SiO_2 mixtures. Red circles are ND70_5_02 and ND70_6_02. Dashed line is the calibration line based on oxalic acid and SiO_2.*

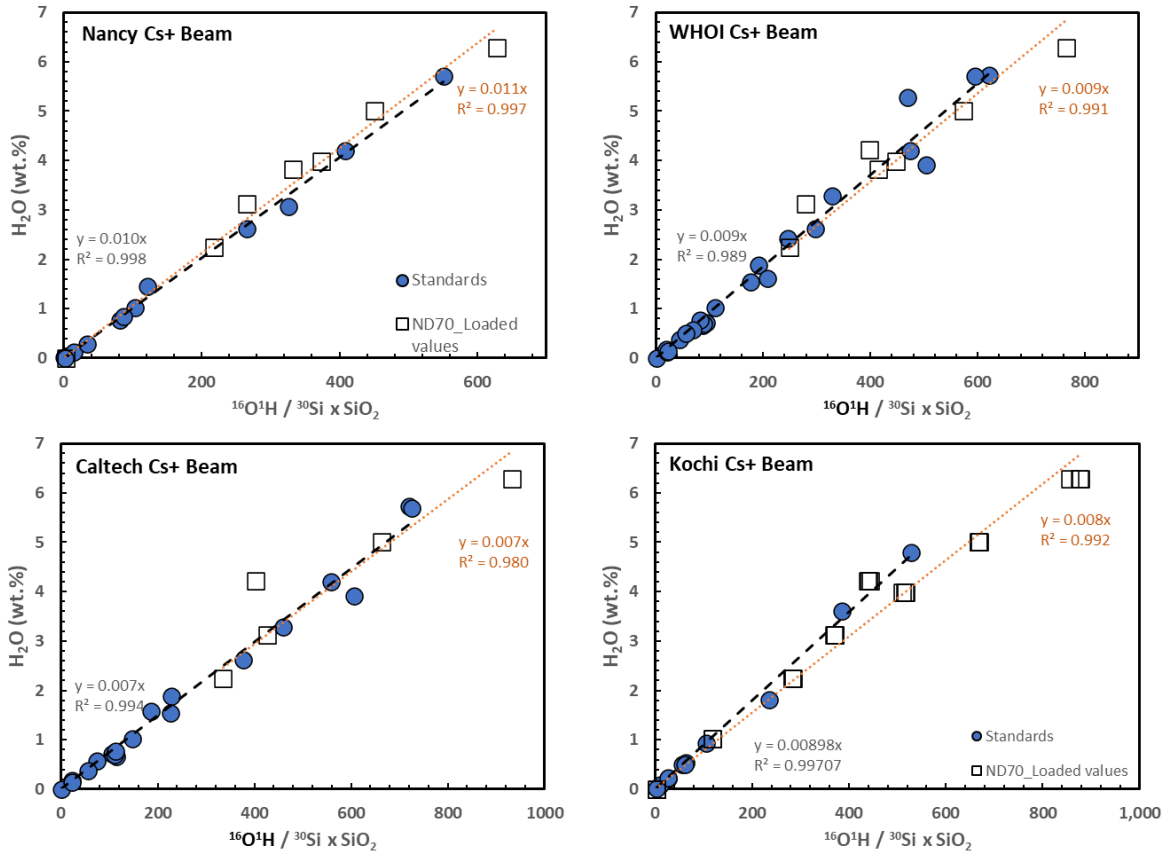

951

952 ***Figure S2***: *$^{16}O^{1}H$ signal retrieved by SIMS using a Cs^{+} primary beam at Nancy, Kochi,*
953 *WHOI and Caltech Ion Probe facilities. Filled circle symbols show glasses used as standards*
954 *for volatile analyses (marked as "Other glasses analysed" in Table 5) in addition to*
955 *INSOL_MX1_BA and VILLA_YM whose volatile contents were determined as part of this*
956 *study. Square symbols represent the new ND70 reference series plotted on the y-axes*
957 *according to their expected (i.e., loaded) values. Data in Tables S3 to S5. Black dashed lines*
958 *are the calibration lines while red dotted lines are linear regressions through the ND series*
959 *glasses.*

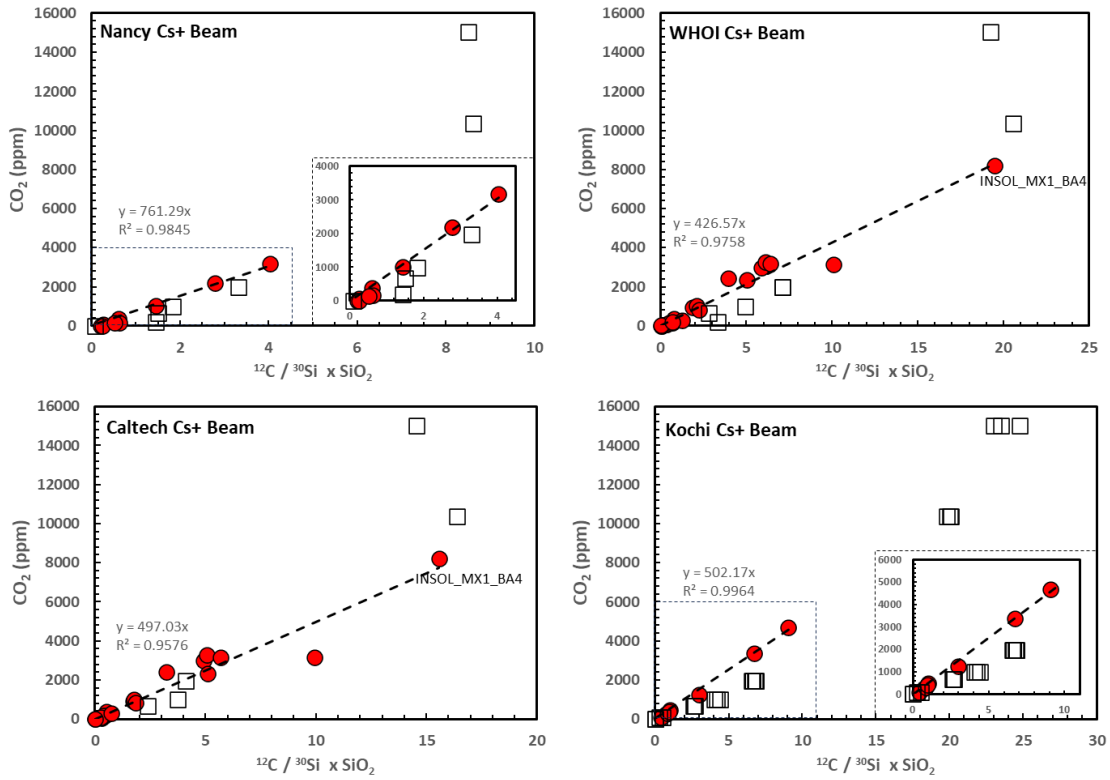

960

961 ***Figure S3**: Same as Fig. S2, for ^{12}C.*

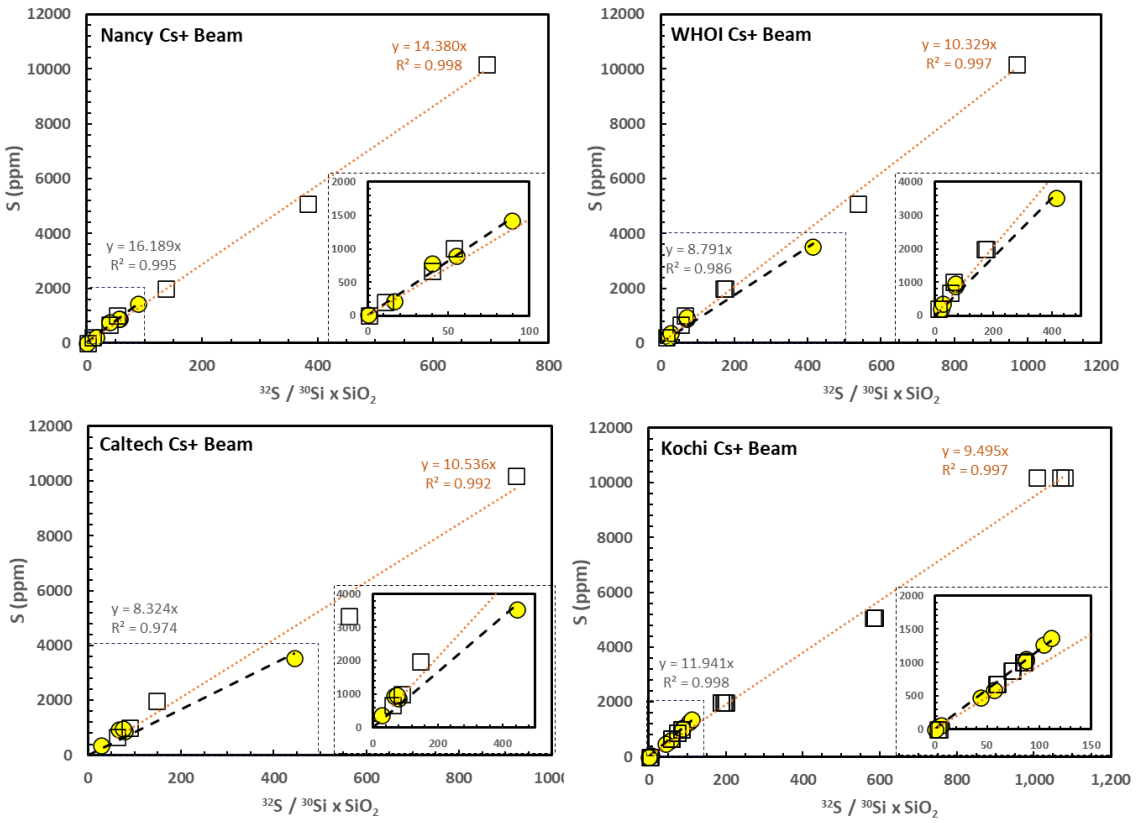

962

963 ***Figure S4****: Same as Fig. S2, for* ^{32}S.

964

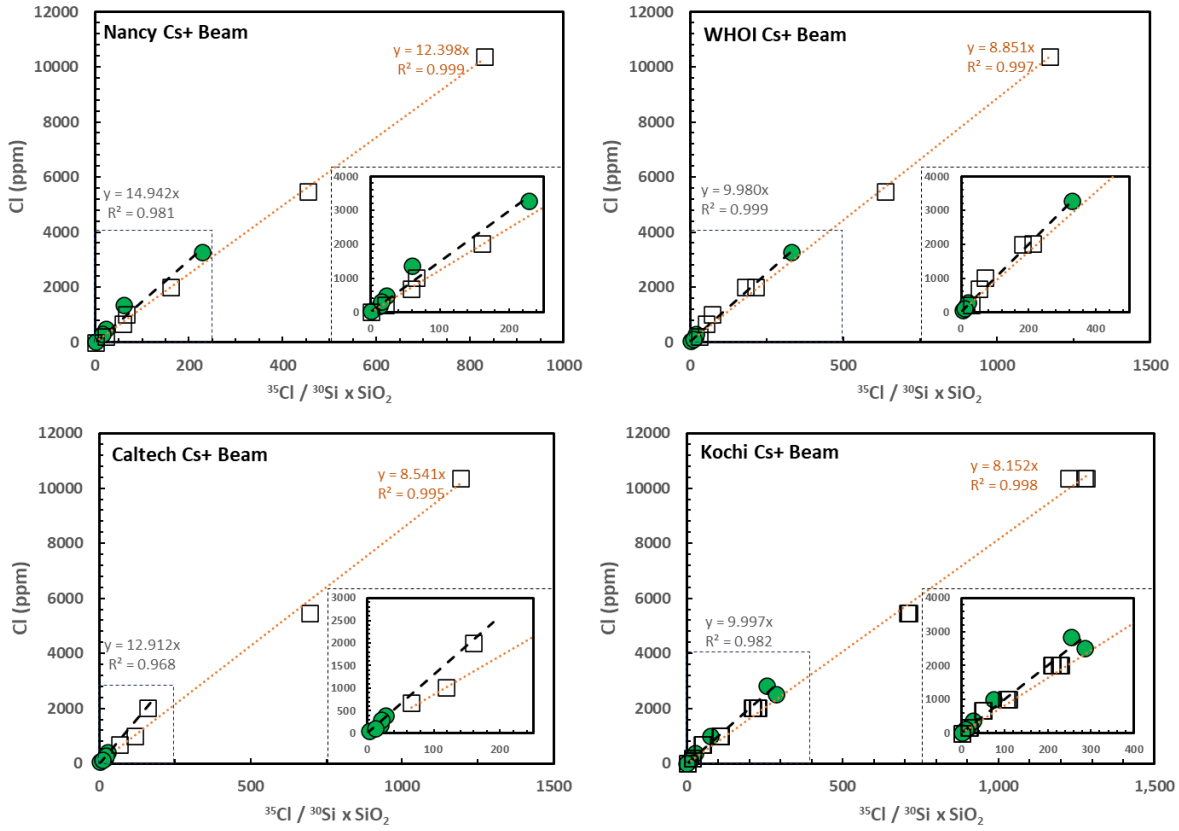

965

966 ***Figure S5****: Same as Fig. S2, for* ^{35}Cl.

967

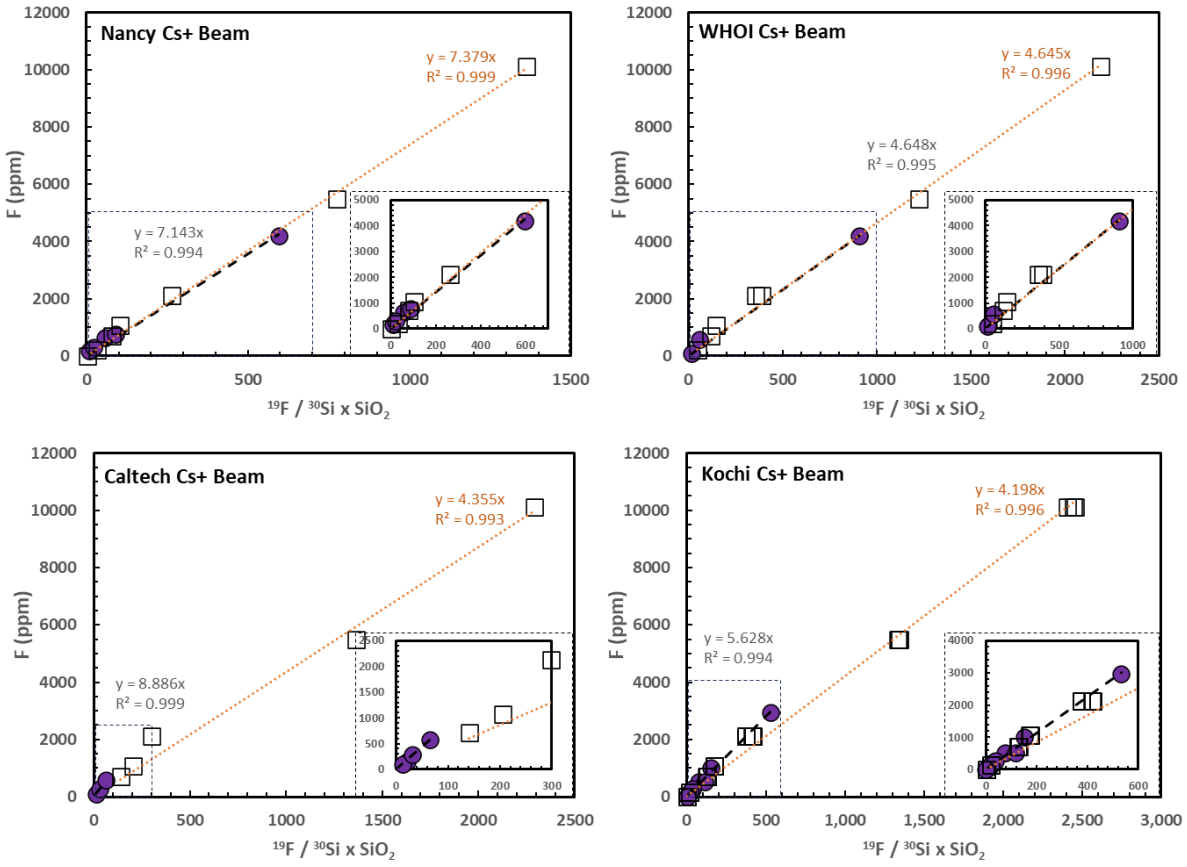

968

969 ***Figure S6****: Same as Fig. S2, for* ^{19}F.

970

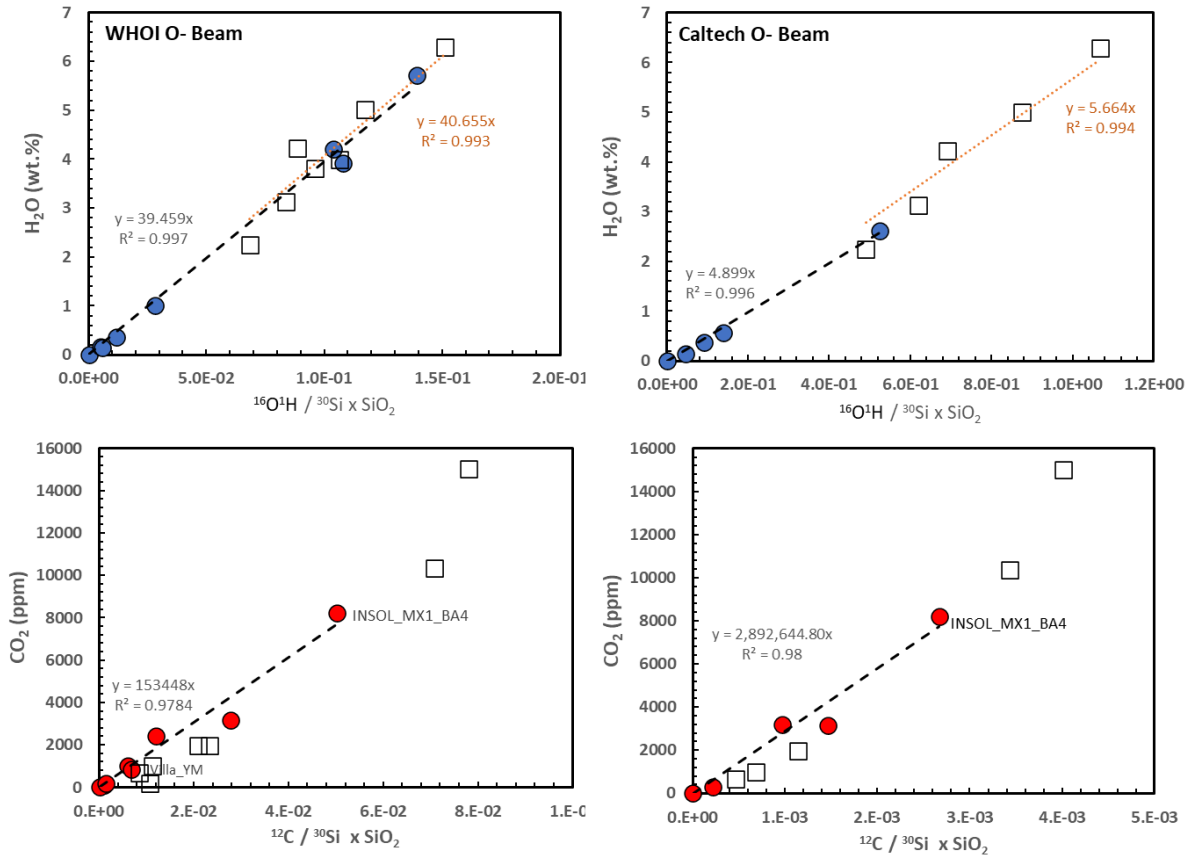

971

972 ***Figure S7****: Signal retrieved by SIMS using a O⁻ primary beam at WHOI and Caltech Ion*
973 *Probe facilities. Filled circle symbols show glasses used as standards for volatile analyses*
974 *(marked as "Other glasses analysed" in Table 5) in addition to INSOL_MX1_BA and*
975 *VILLA_YM whose volatile contents were determined as part of this study. Square symbols*
976 *represent the new ND70 reference series plotted on the y-axes according to their expected*
977 *(i.e., loaded) values. Data in Tables S6 and S7. Black dashed lines are the calibration lines*
978 *while red dotted lines are linear regressions through the ND series glasses.*

979

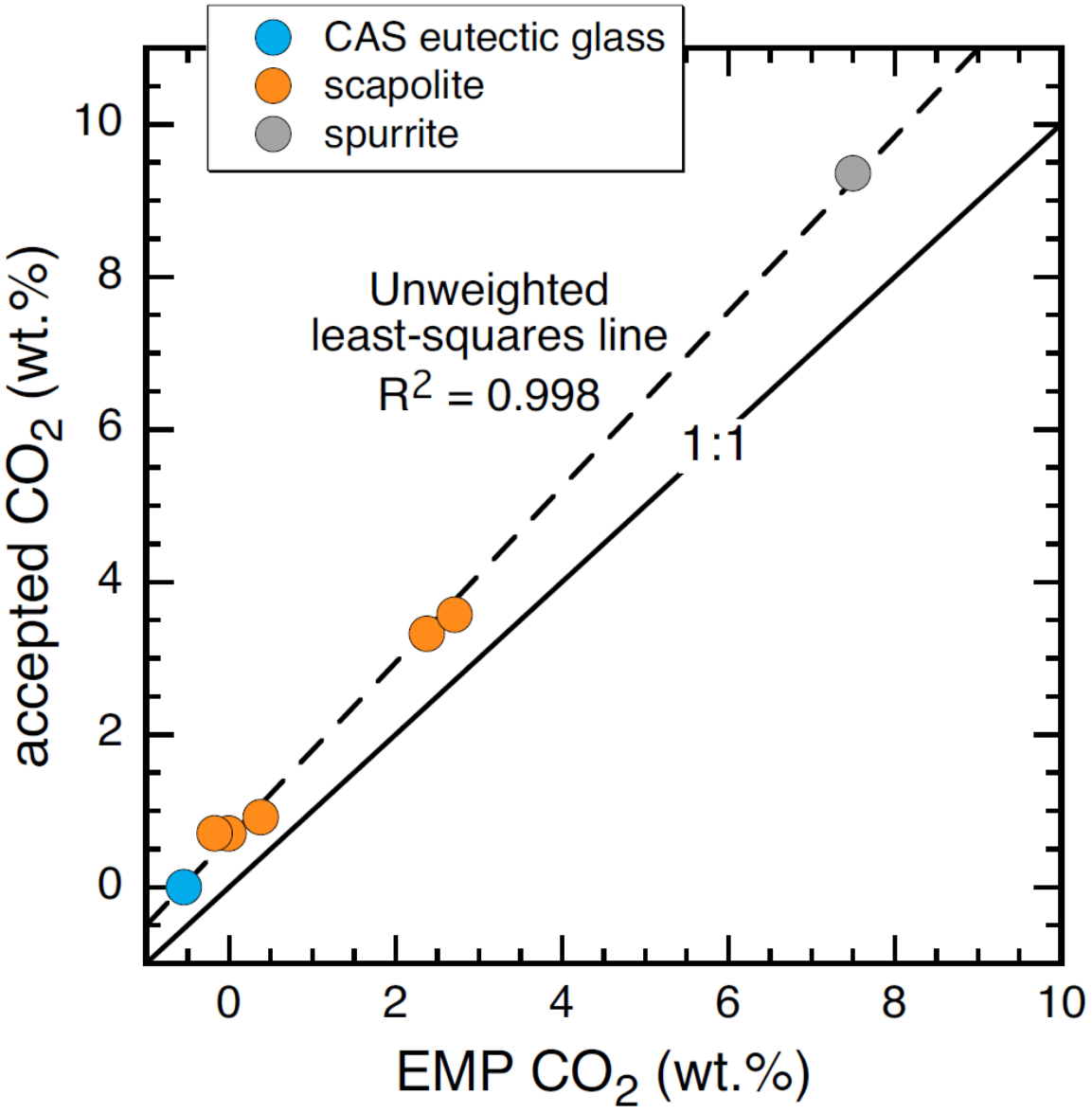

***Figure S8**: Electron microprobe CO_2 contents vs. accepted CO_2 contents (all in wt.%) for the secondary standards. The CaO-Al_2O_3-SiO_2 eutectic is bounded by the pseudowollastonite, anorthite, and tridymite liquidus fields; the glass was fused at 1-atm in air and is assumed to have a CO_2 content of zero. Scapolite CO_2 contents determined by NRA; the CO_2 content of the spurrite is based on mineral stoichiometry. The dashed line is an unweighted least-squares fit to the seven secondary standards.*

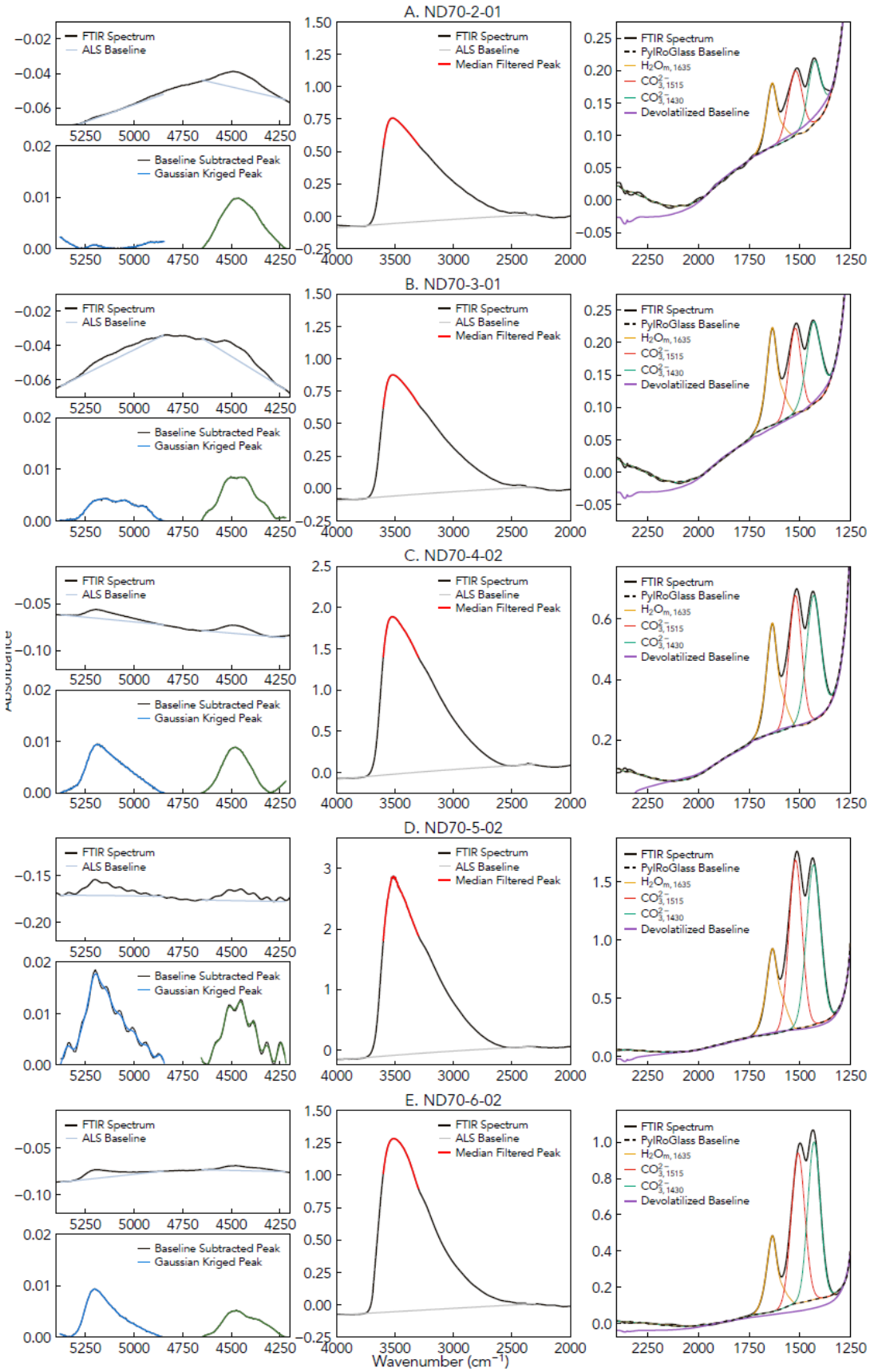

***Figure S9**: FTIR spectra of ND70 series glasses and spectra fitting with the PyIRoGlass software* (Shi et al., 2023).

SUPPLEMENTARY TABLES

Table S1*: Weight of all starting materials added to each experiment. 'ND70-4 Bulk Enriched' is a mixture of all the dry components, mixed for 1 hour, and used as starting material for five of the experiments.*

Experiments and pre-mix	ND70 mix (g)	ND70-4 Bulk Enriched (g)	ND70 + 6wt% SiO2 Mix (g)	Water (g)	Calcite (g)	$CaSO_4$ (g)	NaCl (g)	MgF_2 (g)	Total (g)
ND70-4 Bulk Enriched	0.56770				0.00270	0.00510	0.00200	0.00210	0.57960
ND70-4-01		0.19200		0.00790					0.19990
ND70-4-02		0.19280		0.00840					0.20120
ND70-3-01	0.07310	0.07320		0.00470					0.15100
ND70-2-01	0.13080	0.06550		0.00450					0.20080
ND70-5-03	0.12468	0.01400		0.00550					0.14418
ND70-5-02			0.17790	0.01000	0.00470	0.00430	0.00180	0.00180	0.20050
ND70-6-02			0.16615	0.01250	0.00680	0.00860	0.00340	0.00330	0.20075

998 ***Table S2****: Volatile and SiO_2 contents (normalised to 100%) of other glasses analysed.*

Name	H_2O (wt.%)	CO_2 (ppm)	F (ppm)	S (ppm)	Cl (ppm)	SiO_2 (wt.%)	References
ND-70	1.015	76.5	148	880	184	50.4	Keller et al., 2008; Caulfield et al., 2012; Lloyd et al., 2013
Suprasil	0.0007±0.0002	0.65±0.35	0.19±0.05	0.15±0.03	1000-3000	100.0	Shimizu et al., 2021
BF73	0.72	2995				51.2	Brounce et al., 2021 and Almeev (unpublished)
BF76	0.67	2336				51.2	Brounce et al., 2021 and Almeev (unpublished)
BF77	0.70	935				51.2	Brounce et al., 2021 and Almeev (unpublished)
M15	1.54	60				50.5	Shishkina et al., 2010
M19	3.29	3277				50.4	Shishkina et al., 2010
M20	5.72	2421				50.4	Shishkina et al., 2010
M34	5.70	375				50.4	Shishkina et al., 2010
M35	4.20	1019				50.4	Shishkina et al., 2010
M40	3.07	2183				50.3	Shishkina et al., 2010
M43	2.62	3172				50.4	Shishkina et al., 2010
M48	0.77	176				51.0	Shishkina et al., 2010
KL2	0.02	5	177	8	26	50.1	Jochum et al., 2006; Rose-Koga et al., 2020
KE12	0.12		4200	210	3280	70.8	Mosbah et al., 1991 and Mandeville (unpublished); Rose-Koga et al., 2020
40428	0.85		650	890	494	51.0	Kamenetsky et al., 2000
47963	1.45		777	776	1356	48.9	Kamenetsky et al., 2000
N72	0.00	0				50.1	Shishkina et al., 2010
ALV519-4-1	0.17	165	95	950	53	49.1	Bryan & Moore, 1977; Hauri et al., 2002; Kumamoto et al., 2017 and Hauri (unpublished)
1846-12	1.58	90	288	981	400	50.8	Newman et al., 2000; Hauri et al., 2002; Kumamoto et al., 2017
80-1-3	0.57	295				48.9	Newman et al., 2000
1846-9	1.89	0	574	358	292	49.7	Newman et al., 2000; Kumamoto et al., 2017 and Hauri (unpublished)

NS-1	0.37	3154				50.4	Helo et al., 2011
VILLA_P2	3.92	835		3529	120	53.4	This study
INSOL_MX1_BA4	0.15	8207				52.6	This study
VG2	0.28	153	300	1424	298	50.8	Jarosewich et al., 1980; Rose-Koga et al., 2020
Run101	1.62					57.6	Mandeville et al., 2002
Run10	5.28					57.2	Mandeville et al., 2002
Vol-std-G_EPR-G3	0.22	269	147	1270	159	50.2	Shimizu et al., 2017
Vol-std-G_IND-G1	0.50	97	216	1048	97	50.1	Shimizu et al., 2017
Vol-std-G_Vol-3A	3.60		2957		2833	53.4	Shimizu et al., 2017
Vol-std-G_Vol-1B	0.94	4686	1018	592	1000	50.5	Shimizu et al., 2017
Vol-std-G_Vol-05A	0.54	3354	511	469	376	50.5	Shimizu et al., 2017
Vol-std-G_Vol-005B	0.10	479	55	51	55	49.8	Shimizu et al., 2017
Vol-std-G_MRN-G1	1.81		507	62	2517	70.2	Shimizu et al., 2017
Vol-std-G_MA42	4.79	1243				51.8	Shimizu et al., 2017
Vol-std-G_FJ-G2	0.23	307	151	1372	118	49.6	Shimizu et al., 2017
Vol-std-G_IND-G2	0.50	389	264	1023	113	50.3	Shimizu et al., 2017
Vol-std-G_vol-0B	0.02		8	1	12	48.4	Shimizu et al., 2017

999

1000 ***Table S3****: Raw SIMS analyses from IMS 1280 at CNRS-CRPG Nancy using a Cs+ primary beam. All errors are given as one standard deviation*
1001 *on repeat analyses or as one standard deviation from analytical error (whichever is the highest).*

	SIMS (CNRS-Nancy) Cs+ primary beam																				
Experiment #	n	$^{12}C/^{30}Si$	±	$^{16}O^{1}H/^{30}Si$	±	$^{19}F/^{30}Si$	±	$^{32}S/^{30}Si$	±	$^{35}Cl/^{30}Si$	±	$^{12}C/^{18}O$	±	$^{16}O^{1}H/^{18}O$	±	$^{19}F/^{18}O$	±	$^{32}S/^{18}O$	±	$^{35}Cl/^{18}O$	±
ND 70_ Degassed	2	0.0017	0.0002	0.0578	0.0012	0.0371	0.0022	0.0206	0.0010	0.0048	0.0003	0.0019	0.0001	0.0641	0.0016	0.0403	0.0004	0.0225	0.0001	0.0053	0.0000
ND70-2-01	3	0.0301	0.0024	4.3713	0.1936	1.6094	0.1119	0.8055	0.0434	1.1781	0.0666	0.0265	0.0006	3.9555	0.0437	1.4228	0.0162	0.7207	0.0029	1.0494	0.0045
ND70-3-01	2	0.0370	0.0029	5.3718	0.2615	2.1066	0.1490	1.0753	0.0591	1.3283	0.0789	0.0334	0.0006	4.9536	0.0399	1.9056	0.0232	0.9821	0.0036	1.2108	0.0038
ND70-4-01	2	0.0659	0.0052	7.4514	0.3509	5.2887	0.3632	2.7161	0.1416	3.2016	0.1763	0.0509	0.0010	5.8959	0.0509	4.1039	0.0434	2.1256	0.0139	2.5017	0.0109
ND70-5-02	2	0.1716	0.0156	8.9640	0.5286	15.4225	1.2157	7.6321	0.4503	9.0217	0.5759	0.1291	0.0034	6.9094	0.0465	11.6824	0.1666	5.8729	0.0246	6.8998	0.0253
ND70-5-03	2	0.0287	0.0022	6.6193	0.2875	0.6352	0.0416	0.2154	0.0106	0.4339	0.0231	0.0230	0.0004	5.4222	0.0601	0.5123	0.0051	0.1751	0.0013	0.3521	0.0015
ND70-6-02	2	0.1731	0.0144	12.7743	0.7299	27.6741	2.1188	14.0800	0.7245	16.8742	1.0217	0.1176	0.0026	8.8323	0.0859	18.8701	0.2968	9.7299	0.1092	11.6021	0.0616
Other glasses analyzed																					
ND-70 (Natural)	1	0.0051	0.0004	2.0414	0.0575	0.2716	0.0160	1.1220	0.0501	0.2579	0.0123	0.0047	0.0001	1.9267	0.0418	0.2528	0.0024	1.0512	0.0068	0.2413	0.0014
M34	3	0.0119	0.0008	10.9312	0.3698	0.2182	0.0117	0.0140	0.0007	0.0473	0.0024	0.0075	0.0002	6.9359	0.0813	0.1370	0.0012	0.0088	0.0001	0.0297	0.0003
M35	10	0.0287	0.0023	8.1092	0.3131	0.2083	0.0132	0.0133	0.0009	0.0433	0.0026	0.0191	0.0005	5.5323	0.0789	0.1401	0.0016	0.0089	0.0001	0.0292	0.0002
M40	10	0.0553	0.0038	6.4981	0.2218	0.2035	0.0119	0.0146	0.0008	0.0433	0.0023	0.0390	0.0008	4.6534	0.0716	0.1441	0.0014	0.0103	0.0001	0.0307	0.0002
M43	1	0.0801	0.0052	5.2770	0.1683	0.1883	0.0105	0.0060	0.0004	0.0384	0.0017	0.0591	0.0009	3.9509	0.0685	0.1395	0.0010	0.0044	0.0001	0.0286	0.0002
M48	10	0.0123	0.0012	1.5927	0.0447	0.1759	0.0114	0.0030	0.0003	0.0367	0.0023	0.0104	0.0004	1.3923	0.0358	0.1510	0.0017	0.0025	0.0001	0.0316	0.0002
KL2	10	0.0041	0.0004	0.0219	0.0007	0.1619	0.0110	0.0070	0.0004	0.0182	0.0012	0.0039	0.0002	0.0213	0.0005	0.1548	0.0022	0.0067	0.0001	0.0175	0.0002
KE12	10	0.0021	0.0003	0.2162	0.0098	8.4050	0.6110	0.2303	0.0118	3.2320	0.1966	0.0019	0.0001	0.2081	0.0025	7.9613	0.1329	0.2217	0.0017	3.0826	0.0170
40428	9	0.0066	0.0006	1.6951	0.0724	1.1336	0.0846	1.0777	0.0625	0.4579	0.0286	0.0067	0.0002	1.7806	0.0228	1.1611	0.0170	1.1142	0.0033	0.4723	0.0021
47963	10	0.0061	0.0005	2.4869	0.1206	1.8266	0.1300	0.8160	0.0479	1.2350	0.0758	0.0063	0.0002	2.5894	0.0262	1.8830	0.0251	0.8410	0.0027	1.2689	0.0061
N72	5	0.0049	0.0005	0.0335	0.0008	0.2143	0.0114	0.0047	0.0004	0.0380	0.0018	0.0040	0.0002	0.0281	0.0007	0.1762	0.0016	0.0039	0.0001	0.0314	0.0002
VG2	10	0.0102	0.0008	0.6600	0.0183	0.4403	0.0292	1.7624	0.0888	0.3069	0.0169	0.0098	0.0003	0.6536	0.0163	0.4263	0.0054	1.7223	0.0081	0.2989	0.0009

1002
1003
1004

***Table S4**: Raw SIMS analyses from IMS 7f-GEO at Caltech using a Cs+ primary beam. All errors are given as one standard from analytical error.*

	SIMS (Caltech) Cs+ primary beam																			
Experiment #	n	$^{12}C/^{30}Si$	±	$^{16}O^{1}H/^{30}Si$	±	$^{19}F/^{30}Si$	±	$^{32}S/^{30}Si$	±	$^{35}Cl/^{30}Si$	±	$^{12}C/^{18}O$	±	$^{16}O^{1}H/^{18}O$	±	$^{19}F/^{18}O$	±	$^{32}S/^{18}O$	±	$^{35}Cl/^{18}O$	±
ND70-2-01	2	0.0478	0.0002	6.7317	0.0170	2.8197	0.0226	1.2384	0.0183	1.3360	0.0411	0.0274	0.0002	3.8655	0.0188	1.6202	0.0175	0.7144	0.0123	0.7708	0.0255
ND70-3-01	8	0.0752	0.0054	8.6127	0.3426	4.1524	0.1505	1.8058	0.0625	2.3865	0.0928	0.0391	0.0013	4.5398	0.2608	2.1764	0.0452	0.9468	0.0357	1.2517	0.0445
ND70-4-02	3	0.0843	0.0035	8.2648	0.2507	6.1457	0.2329	3.0092	0.0691	3.2802	0.0749	0.0584	0.0009	5.7656	0.0102	4.2917	0.0403	2.1238	0.0137	2.3185	0.0307
ND70-5-02	2	0.3262	0.0021	13.2015	0.1969	27.1263	0.0998	11.2017	0.0430	13.7957	0.1175	0.1476	0.0007	6.0019	0.1567	12.3280	0.1835	5.1213	0.0792	6.3053	0.1274
ND70-6-02	2	0.2958	0.0164	18.9729	1.2590	46.5657	2.3499	18.7704	0.2025	24.2523	0.3967	0.1269	0.0022	8.1747	0.2270	20.0705	0.2322	8.1458	0.2286	10.5244	0.2328
Other glasses analysed																					
ND-70 (Natural)	2	0.0054	0.0001	2.9097	0.1264	0.4307	0.0127	1.5644	0.0070	0.3944	0.0239	0.0033	0.0000	1.7813	0.0463	0.2637	0.0030	0.9605	0.0215	0.2420	0.0102
Suprasil	2	0.0000	0.0000	0.0013	0.0000	0.0002	0.0000	0.0000	0.0000	1.9023	0.0447	0.0000	0.0000	0.0008	0.0000	0.0001	0.0000	0.0000	0.0000	1.2669	0.0439
BF73	2	0.0957	0.0020	2.0744	0.0498	0.1612	0.0021	0.0001	0.0000	0.0798	0.0004	0.0602	0.0005	1.3135	0.0162	0.1015	0.0000	0.0001	0.0000	0.0503	0.0004
BF76	2	0.0996	0.0062	2.2367	0.1879	0.1336	0.0086	0.0003	0.0001	0.0815	0.0029	0.0570	0.0014	1.2869	0.0571	0.0764	0.0019	0.0002	0.0000	0.0467	0.0003
BF77	2	0.0335	0.0016	2.1690	0.1154	0.1254	0.0049	0.0006	0.0000	0.0773	0.0033	0.0205	0.0005	1.3339	0.0408	0.0766	0.0012	0.0004	0.0000	0.0473	0.0010
M15	2	0.0055	0.0003	4.4695	0.0615	0.2567	0.0040	0.0015	0.0003	0.0486	0.0004	0.0032	0.0001	2.5973	0.0324	0.1492	0.0016	0.0009	0.0001	0.0283	0.0005
M19	2	0.1005	0.0002	9.0987	0.0086	0.2719	0.0064	0.0076	0.0006	0.0532	0.0030	0.0540	0.0007	4.8984	0.0450	0.1465	0.0019	0.0041	0.0003	0.0288	0.0013
M20	2	0.0642	0.0010	14.2935	0.0897	0.2936	0.0007	0.0201	0.0003	0.0594	0.0001	0.0287	0.0003	6.4065	0.0023	0.1316	0.0005	0.0090	0.0002	0.0266	0.0001
M34	1	0.0106	0.0002	14.3829	0.1797	0.2767	0.0040	0.0135	0.0003	0.0530	0.0013	0.0051	0.0001	6.9973	0.0547	0.1347	0.0009	0.0066	0.0001	0.0258	0.0004
M35	2	0.0347	0.0021	11.0667	0.9776	0.2818	0.0101	0.0113	0.0001	0.0527	0.0001	0.0169	0.0007	5.3833	0.3833	0.1373	0.0024	0.0055	0.0002	0.0258	0.0005
M43	1	0.1132	0.0018	7.4751	0.0851	0.2707	0.0047	0.0041	0.0001	0.0541	0.0012	0.0604	0.0003	3.9914	0.0142	0.1445	0.0008	0.0022	0.0000	0.0289	0.0003
M48	1	0.0087	0.0001	2.2129	0.0203	0.2501	0.0034	0.0001	0.0000	0.0465	0.0009	0.0054	0.0001	1.3672	0.0064	0.1545	0.0006	0.0001	0.0000	0.0288	0.0003
ALV519-4-1	2	0.0077	0.0007	0.4490	0.0260	0.2550	0.0104	1.3248	0.0014	0.0734	0.0003	0.0059	0.0003	0.3438	0.0072	0.1951	0.0006	1.0234	0.0385	0.0567	0.0025
1846-12	2	0.0050	0.0001	3.6540	0.0268	0.6252	0.0128	1.4597	0.0264	0.5293	0.0107	0.0034	0.0000	2.4897	0.0160	0.4257	0.0024	1.0009	0.0026	0.3631	0.0017
80-1-3	2	0.0150	0.0011	1.5076	0.0055	0.7287	0.0087	1.3904	0.0159	0.0952	0.0012	0.0104	0.0009	1.0467	0.0104	0.5050	0.0003	0.9694	0.0224	0.0663	0.0016
1846-9	2	0.0003	0.0000	4.6133	0.1971	1.3004	0.0560	0.5399	0.0081	0.4284	0.0065	0.0002	0.0000	2.8100	0.0058	0.7901	0.0019	0.3305	0.0083	0.2625	0.0066
NS-1	3	0.1969	0.0106	1.1232	0.0394	0.3005	0.0064	0.0758	0.0034	0.0548	0.0033	0.1216	0.0048	0.6996	0.0155	0.1861	0.0048	0.0472	0.0025	0.0341	0.0023
VILLA_P2	2	0.0344	0.0024	11.4049	0.3284	0.6406	0.0226	8.3473	0.3511	0.2201	0.0090	0.0165	0.0006	5.6285	0.0236	0.3084	0.0011	4.1159	0.3091	0.1063	0.0010
INSOL_MX1_BA4	2	0.2957	0.0073	0.4497	0.0080	1.0520	0.0288	0.0128	0.0007	0.1404	0.0022	0.2117	0.0021	0.3262	0.0056	0.7595	0.0052	0.0094	0.0008	0.1026	0.0018

1007

1008 ***Table S5****: Raw SIMS analyses from IMS 1280 at WHOI using a Cs+ primary beam. All errors are given as one standard from analytical error.*

	SIMS (WHOI) Cs+ primary beam									
Experiment #	n	12C/30Si	±	16O1H/30Si	±	19F /30Si	±	32S /30Si	±	35Cl /30Si	±
ND70-2-01	3	0.0567	0.0013	4.9908	0.0825	2.3760	0.0294	1.0878	0.0068	1.0433	0.0213
ND70-3-01	2	0.0997	0.0029	5.6332	0.1643	2.9645	0.1933	1.3357	0.1003	1.4319	0.1657
ND70-4-01	3	0.1419	0.0023	8.9285	0.0868	7.7497	0.0527	3.5208	0.0274	4.2429	0.0406
ND70-4-02	3	0.1458	0.0010	8.1725	0.0150	7.3624	0.0271	3.5184	0.0232	3.7283	0.0346
ND70-5-02	3	0.4089	0.0086	11.3843	0.2507	24.3667	0.2252	10.6667	0.0273	12.6703	0.1309
ND70-5-03	3	0.0658	0.0010	8.2423	0.1151	0.9277	0.0155	0.2896	0.0039	0.5979	0.0132
ND70-6-02	3	0.3915	0.0024	15.5580	0.3396	44.5050	0.4786	19.7107	0.2466	23.8557	0.4052
Other glasses analysed											
ND-70 (Natural)	3	0.0056	0.0001	2.1747	0.0161	0.3684	0.0028	1.4098	0.0059	0.3185	0.0018
Suprasil	3	0.0006	0.0009	0.0078	0.0021	0.0075	0.0002	0.0002	0.0002	1.9159	0.0178
BF73	2	0.1145	0.0093	1.8283	0.0315	0.1505	0.0009	0.0006	0.0007	0.0708	0.0009
BF76	2	0.0977	0.0009	1.7173	0.0153	0.1142	0.0002	0.0004	0.0001	0.0675	0.0003
BF77	3	0.0362	0.0002	1.7300	0.0153	0.1140	0.0009	0.0007	0.0000	0.0662	0.0006
M15	3	0.0071	0.0012	3.5002	0.0535	0.2273	0.0016	0.0016	0.0001	0.0414	0.0006
M19	3	0.1212	0.0029	6.5289	0.0298	0.2316	0.0015	0.0064	0.0003	0.0414	0.0009
M20	3	0.0785	0.0020	12.3073	0.1822	0.2660	0.0026	0.0176	0.0003	0.0499	0.0012
M34	3	0.0155	0.0027	11.7937	0.0590	0.2563	0.0012	0.0125	0.0002	0.0479	0.0005
M35	3	0.0417	0.0013	9.4117	0.0320	0.2542	0.0031	0.0105	0.0003	0.0472	0.0007
M43	3	0.1266	0.0008	5.9117	0.0665	0.2360	0.0010	0.0037	0.0000	0.0450	0.0010
M48	3	0.0137	0.0073	1.6145	0.0207	0.2119	0.0017	0.0003	0.0002	0.0382	0.0007
KE12	3	0.0002	0.0001	0.3022	0.0169	12.8230	0.0459	0.3286	0.0102	4.6523	0.0382
ALV519-4-1	5	0.0098	0.0001	0.4117	0.0044	0.2708	0.0025	1.4244	0.0153	0.0802	0.0015
80-1-3	3	0.0255	0.0098	1.3997	0.0357	0.7085	0.0095	1.3856	0.0028	0.0955	0.0025
NS-1	3	0.1999	0.0077	0.8877	0.0229	0.2543	0.0028	0.0694	0.0009	0.0482	0.0006
VILLA_P2	3	0.0416	0.0012	9.4519	0.0758	0.5811	0.0041	7.7760	0.6566	0.1994	0.0036

INSOL_MX1_BA4	3	0.3703	0.0102	0.4441	0.0574	1.1063	0.0570	0.0176	0.0045	0.1534	0.0106
Run101@2.asc	3	0.0022	0.0001	3.6113	0.0404	1.0030	0.0281	0.5635	0.0188	0.9911	0.0370
Run10@2.asc	3	0.0009	0.0001	8.1861	0.1171	0.0166	0.0005	0.0400	0.0016	0.7018	0.0189
ALV_1846-9	4	0.0004	0.0000	3.8590	0.0445	1.1673	0.0093	0.5410	0.0053	0.4149	0.0064
ALV_1833-1	3	0.0007	0.0000	4.5644	0.1128	1.0142	0.0067	1.0499	0.0241	1.0283	0.0224
WOK28-3	3	0.0137	0.0002	1.1325	0.0089	0.4112	0.0025	1.4849	0.0155	0.0901	0.0012

1011 ***Table S6****: Raw SIMS analyses from IMS 7f-GEO at Caltech using a O- primary beam. All errors are given as one standard from analytical*
1012 *error.*

	SIMS (Caltech) O- primary beam				
Experiment #	n	$^{12}C/^{30}Si$	±	$^{16}O^{1}H/^{30}Si$	±
ND70-2-01	2	9.32E-06	1.25E-07	9.86E-03	1.11E-04
ND70-3-01	2	1.38E-05	1.43E-06	1.25E-02	1.11E-04
ND70-4-02	2	2.35E-05	1.90E-06	1.42E-02	2.97E-04
ND70-5-02	2	6.83E-05	5.76E-07	1.74E-02	1.59E-04
ND70-6-02	2	8.16E-05	2.48E-07	2.17E-02	6.33E-04
Other glasses analysed					
Suprasil	1	0.00E+00	2.07E-06	0.00E+00	1.53E-08
M43	2	1.93E-05	2.99E-07	1.04E-02	9.22E-06
80-1-3	1	4.42E-06	1.69E-07	2.84E-03	1.05E-05
NS-1	2	2.90E-05	4.28E-07	1.82E-03	1.83E-04
INSOL_MX1_BA4	1	5.08E-05	1.12E-05	8.93E-04	2.52E-07

1013

1014 ***Table S7****: Raw SIMS analyses from IMS 1280 at WHOI using a O- primary beam. All errors are given as one standard from analytical error.*

	SIMS (WHOI) O- primary beam										
Experiment #	n	12C/30Si	±	16O1H/30Si	±	19F /30Si	±	32S /30Si	±	35Cl /30Si	±
ND70-2-01	3	1.72E-04	4.14E-06	1.37E-03	1.09E-05	2.42E-02	2.08E-04	1.56E-03	1.73E-05	5.49E-04	5.16E-06
ND70-3-01	5	2.26E-04	1.20E-05	1.70E-03	3.89E-05	3.44E-02	2.91E-04	1.86E-03	1.92E-05	9.77E-04	2.01E-05
ND70-4-01	5	4.67E-04	1.13E-05	2.12E-03	4.06E-05	6.83E-02	6.44E-04	2.90E-03	5.77E-05	1.93E-03	4.47E-05
ND70-4-02	3	4.31E-04	5.71E-06	1.82E-03	2.31E-05	6.22E-02	5.18E-04	2.82E-03	9.30E-06	1.61E-03	2.41E-05
ND70-5-02	3	1.41E-03	2.04E-05	2.33E-03	7.00E-05	1.90E-01	5.93E-03	6.40E-03	1.38E-04	5.11E-03	2.39E-04
ND70-5-03	3	2.15E-04	1.88E-06	1.91E-03	1.44E-05	8.23E-03	1.69E-04	9.08E-04	8.60E-06	2.74E-04	3.87E-06
ND70-6-02	3	1.59E-03	1.99E-05	3.07E-03	1.44E-04	3.65E-01	1.20E-02	1.10E-02	5.96E-04	1.04E-02	6.60E-04
Other glasses analysed											
ND-70 (Natural)	3	2.10E-05	2.16E-06	5.64E-04	1.76E-05	3.63E-03	6.44E-05	1.73E-03	3.48E-05	1.73E-04	4.53E-06
Suprasil	3	1.97E-06	6.47E-07	2.43E-06	1.05E-06	1.64E-06	5.55E-07	4.60E-07	1.71E-07	3.01E-04	1.99E-05
M20	3	2.39E-04	2.30E-06	2.76E-03	8.94E-05	2.04E-03	6.06E-05	6.50E-04	1.64E-05	4.84E-05	2.47E-06
M35	3	1.20E-04	3.70E-06	2.06E-03	1.95E-05	1.93E-03	5.58E-06	5.10E-04	1.47E-05	3.69E-05	1.27E-06
ALV519-4-1	3	2.85E-05	1.02E-06	1.03E-04	4.84E-06	2.65E-03	7.42E-05	1.83E-03	3.79E-05	5.41E-05	5.31E-06
NS-1	3	5.50E-04	7.34E-06	2.40E-04	3.43E-06	2.56E-03	5.11E-05	8.66E-04	2.83E-05	4.02E-05	3.77E-06
VILLA_P2	3	1.27E-04	3.12E-06	2.03E-03	8.22E-05	3.71E-03	1.31E-04	3.17E-03	1.32E-04	7.54E-05	4.91E-06
INSOL_MX1_BA4	3	9.55E-04	9.31E-05	1.15E-04	1.80E-05	1.22E-02	1.87E-03	7.98E-04	4.14E-05	1.10E-04	1.28E-05

1015

1016

***Table S8**: Raw SIMS analyses from IMS 1280 at JAMSTEC Kochi Institute using a Cs+ primary beam. All errors are given as one standard deviation on repeat analyses or as one standard deviation from analytical error (whichever is the highest).*

	SIMS (JAMSTEC-Kochi) Cs+ primary beam										
Experiment #	n	12C/30Si	±	16O1H/30Si	±	19F /30Si	±	32S /30Si	±	35Cl /30Si	±
ND 70_ Degassed	2	**0.0003**	**0.0000**	0.0672	**0.0001**	**0.0581**	0.0019	0.0649	0.0248	**0.0231**	**0.0130**
ND70-2-01	3	**0.0535**	**0.0007**	5.6850	**0.0125**	**2.5715**	0.0211	1.1908	0.0084	**0.9936**	**0.0293**
ND70-3-01	3	**0.0851**	**0.0038**	7.4538	**0.0213**	**3.5139**	0.0345	1.7151	0.0124	**2.1524**	**0.0438**
ND70-4-01	3	**0.1311**	**0.0005**	10.1917	**0.0813**	**8.2971**	0.0472	3.9268	0.0527	**4.5143**	**0.0374**
ND70-4-02	3	**0.1394**	**0.0008**	9.0278	**0.0500**	**7.6666**	0.0085	3.8328	0.0112	**4.3001**	**0.0219**
ND70-5-02	3	**0.3922**	**0.0026**	13.1235	**0.0254**	**26.3081**	0.0764	11.4754	0.0503	**13.9327**	**0.0475**
ND70-6-02	3	**0.4716**	**0.0184**	17.2664	**0.2443**	**48.3145**	0.5284	20.8799	0.7687	**25.0239**	**0.6325**
Other glasses (and minerals) analyzed											
ND-70 (Natural)	2	**0.0079**	**0.0033**	2.3344	**0.0095**	**0.3683**	0.0019	1.4617	0.0058	**0.3477**	**0.0075**
Vol-std-G_EPR-G3	5	**0.0141**	**0.0004**	0.5373	**0.0030**	**0.4153**	0.0020	2.0627	0.0163	**0.2352**	**0.0022**
Vol-std-G_SC-ol	1	**0.0004**	**0.0000**	0.0098	**0.0003**	**0.0057**	0.0001	0.0003	0.0000	**0.0003**	**0.0000**
Vol-std-G_ELA-qz	4	**0.0002**	**0.0002**	0.0058	**0.0013**	**0.0022**	0.0005	0.0002	0.0001	**0.0004**	**0.0001**
Vol-std-G_IND-G1	1	**0.0082**	**0.0001**	1.1270	**0.0036**	**0.6087**	0.0020	1.7418	0.0043	**0.1548**	**0.0006**
Vol-std-G_Vol-3A	1	**0.1786**	**0.0007**	7.2310	**0.0174**	**9.9764**	0.0203	1.6415	0.0404	**4.7743**	**0.0084**
Vol-std-G_Vol-1B	1	**0.1791**	**0.0005**	2.0724	**0.0038**	**2.9762**	0.0046	1.1141	0.0020	**1.4706**	**0.0012**
Vol-std-G_Vol-05A	1	**0.1333**	**0.0006**	1.2576	**0.0042**	**1.4683**	0.0035	0.8625	0.0027	**0.5378**	**0.0012**
Vol-std-G_Vol-005B	1	**0.0201**	**0.0001**	0.2120	**0.0005**	**0.1640**	0.0004	0.0742	0.0004	**0.0637**	**0.0004**
Vol-std-G_MRN-G1	1	**0.0002**	**0.0000**	3.3626	**0.0081**	**1.6462**	0.0044	0.0859	0.0005	**4.0661**	**0.0085**
Vol-std-G_MA42	1	**0.0574**	**0.0004**	10.1889	**0.0263**	**0.2469**	0.0006	0.0468	0.0005	**0.2145**	**0.0008**
Vol-std-G_FJ-G2	1	**0.0172**	**0.0001**	0.5344	**0.0014**	**0.4193**	0.0010	2.2429	0.0039	**0.1808**	**0.0006**
Vol-std-G_IND-G2	1	**0.0191**	**0.0002**	1.2013	**0.0022**	**0.7376**	0.0016	1.7335	0.0047	**0.1593**	**0.0005**
Vol-std-G_vol-0B	1	**0.0003**	**0.0000**	0.0509	**0.0005**	**0.0185**	0.0003	0.0020	0.0001	**0.0012**	**0.0000**

***Table S9**: Data used to generate Figure 8.*

Sample number	SiO_2 (normalized)	CO_2 (ppm)	H_2O	SIMS Cs+ Nancy $^{12}C/^{30}Si$	SIMS Cs+ Nancy $^{12}C/^{18}O$	SIMS Cs+ Kochi $^{12}C/^{30}Si$	SIMS Cs+ WHOI $^{12}C/^{30}Si$	SIMS O- WHOI $^{12}C/^{30}Si$	SIMS Cs+ Caltech $^{12}C/^{30}Si$	SIMS Cs+ Caltech $^{12}C/^{18}O$	SIMS O- Caltech $^{12}C/^{30}Si$	SIMS Cs+ Nancy $(({}^{12}C/{}^{30}Si)x SiO_2)/CO_2$	SIMS Cs+ Nancy $^{12}C/{}^{18}O/CO_2$	SIMS Cs+ Kochi $(({}^{12}C/{}^{30}Si)x SiO_2)/CO_2$	SIMS Cs+ WHOI $(({}^{12}C/{}^{30}Si)x SiO_2)/CO_2$	SIMS O- WHOI $(({}^{12}C/{}^{30}Si)x SiO_2)/CO_2$	SIMS Cs+ Caltech $(({}^{12}C/{}^{30}Si)x SiO_2)/CO_2$	SIMS Cs+ Caltech $^{12}C/{}^{18}O/CO_2$	SIMS O- Caltech $(({}^{12}C/{}^{30}Si)x SiO_2)/CO_2$
ND 70_ Degassed	50.1			1.74E-03	1.86E-03	3.11E-04													
ND70-2-01	49.8	1560	2.4	3.01E-02	2.65E-02	5.35E-02	5.67E-02	1.72E-04	4.78E-02	2.74E-02	9.32E-06	9.61E-04	1.70E-05	1.71E-03	1.81E-03	5.49E-06	1.53E-03	1.76E-05	2.98E-07
ND70-3-01	49.5	2637	3.1	3.70E-02	3.34E-02	8.51E-02	9.97E-02	2.26E-04	7.52E-02	3.91E-02	1.38E-05	6.96E-04	1.27E-05	1.60E-03	1.87E-03	4.25E-06	1.41E-03	1.48E-05	2.59E-07
ND70-4-01	50.2	4161	4.1	6.59E-02	5.09E-02	1.31E-01	1.42E-01	4.67E-04				7.95E-04	1.22E-05	1.58E-03	1.71E-03	5.63E-06			
ND70-4-02	48.7	4214	3.6			1.39E-01	1.46E-01	4.31E-04	8.43E-02	5.84E-02	2.35E-05			1.61E-03	1.68E-03	4.98E-06	9.74E-04	1.39E-05	2.71E-07
ND70-5-02	50.3	12237	5.0	1.72E-01	1.29E-01	3.92E-01	4.09E-01	1.41E-03	3.26E-01	1.48E-01	6.83E-05	7.05E-04	1.05E-05	1.61E-03	1.68E-03	5.78E-06	1.34E-03	1.21E-05	2.80E-07
ND70-6-02	49.2	15847	6.4	1.73E-01	1.18E-01	4.72E-01	3.91E-01	1.59E-03	2.96E-01	1.27E-01	8.16E-05	5.37E-04	7.42E-06	1.46E-03	1.22E-03	4.93E-06	9.18E-04	8.01E-06	2.53E-07
ND-70 (Natural)	50.4	145	1.0	5.09E-03	4.71E-03	7.86E-03	5.60E-03	2.10E-05	5.37E-03	3.29E-03		1.77E-03	3.24E-05	2.73E-03	1.94E-03	7.30E-06	1.86E-03	2.26E-05	
BF73	51.2	2995	0.7				1.15E-01		9.57E-02	6.02E-02					1.96E-03		1.64E-03	2.01E-05	
BF76	51.2	2336	0.7				9.77E-02		9.96E-02	5.70E-02					2.14E-03		2.18E-03	2.44E-05	
BF77	51.2	935	0.7				3.62E-02		3.35E-02	2.05E-02					1.98E-03		1.84E-03	2.19E-05	
M15	50.5	60	1.5				7.08E-03		5.50E-03	3.19E-03					5.95E-03		4.62E-03	5.32E-05	
M19	50.4	3277	3.3				1.21E-01		1.01E-01	5.40E-02					1.87E-03		1.55E-03	1.65E-05	
M20	50.4	2421	5.7				7.85E-02	2.39E-04	6.42E-02	2.87E-02					1.64E-03	4.98E-06	1.34E-03	1.19E-05	
M34	50.4	375	5.7	1.19E-02	7.46E-03		1.55E-02		1.06E-02	5.13E-03		1.61E-03	1.99E-05		2.08E-03		1.42E-03	1.37E-05	
M35	50.4	1019	4.2	2.87E-02	1.91E-02		4.17E-02	1.20E-04	3.47E-02	1.69E-02		1.42E-03	1.88E-05		2.06E-03	5.93E-06	1.72E-03	1.66E-05	
M40	50.3	2183	3.1	5.53E-02	3.90E-02							1.27E-03	1.79E-05						
M43	50.4	3172	2.6	8.01E-02	5.91E-02		1.27E-01		1.13E-01	6.04E-02	1.93E-05	1.27E-03	1.86E-05		2.01E-03		1.80E-03	1.90E-05	3.06E-07
M48	51.0	176	0.8	1.23E-02	1.04E-02		1.37E-02		8.71E-03	5.37E-03		3.56E-03	5.91E-05		3.97E-03		2.52E-03	3.05E-05	
ALV519-4-1	49.1	165	0.2				9.80E-03	2.85E-05	7.74E-03	5.88E-03					2.91E-03	8.49E-06	2.30E-03	3.56E-05	
1846-12	50.8	90	1.6						4.98E-03	3.38E-03							2.81E-03	3.76E-05	

80-1-3	48.9	295	0.6				2.55E-02		1.50E-02	1.04E-02	4.42E-06				4.23E-03		2.49E-03	3.52E-05	7.33E-07	
1846-9	49.7	0	1.9				4.30E-04		2.85E-04	1.72E-04										
NS-1	50.4	3154	0.4				2.00E-01	5.50E-04	1.97E-01	1.22E-01	2.90E-05				3.19E-03	8.79E-06	3.15E-03	3.86E-05	4.63E-07	
Villa_YM	53.2	835	3.9				4.16E-02	1.27E-04	3.44E-02	1.65E-02					2.65E-03	8.12E-06	2.19E-03	1.97E-05		
INSOL_MX1_BA4	52.6	8207	0.2				3.70E-01	9.55E-04	2.96E-01	2.12E-01	5.08E-05				2.37E-03	6.13E-06	1.90E-03	2.58E-05	3.26E-07	
VG2	50.8	153	0.3	1.02E-02	9.80E-03							3.40E-03	6.41E-05							
ALV_1833-1	53.9	24	2.4				6.68E-04								1.50E-03					
WOK28-3	49.8	183	0.5				1.37E-02								3.74E-03					
Vol-std-G_EPR-G3	50.2	269	0.2			1.41E-02								2.63E-03						
Vol-std-G_IND-G1	50.1	97	0.5			8.17E-03								4.22E-03						
Vol-std-G_Vol-1B	50.5	4686	0.9			1.79E-01								1.93E-03						
Vol-std-G_Vol-05A	50.5	3354	0.5			1.33E-01								2.01E-03						
Vol-std-G_Vol-005B	49.8	479	0.1			2.01E-02								2.09E-03						
Vol-std-G_MA42	51.8	1243	4.8			5.74E-02								2.39E-03						
Vol-std-G_FJ-G2	49.6	307	0.2			1.72E-02								2.78E-03						
Vol-std-G_IND-G2	50.3	389	0.5			1.91E-02								2.47E-03						

REFERENCES

Brounce, M., Reagan, M. K., Kelley, K. A., Cottrell, E., Shimizu, K., & Almeev, R. (2021). Covariation of Slab Tracers, Volatiles, and Oxidation During Subduction Initiation. *Geochemistry, Geophysics, Geosystems*, *22*(6), e2021GC009823. https://doi.org/10.1029/2021GC009823

Bryan, W. B., & Moore, J. G. (1977). Compositional variations of young basalts in the Mid-Atlantic Ridge rift valley near lat 36°49′N. *GSA Bulletin*, *88*(4), 556–570. https://doi.org/10.1130/0016-7606(1977)88<556:CVOYBI>2.0.CO;2

Caulfield, J., Turner, S., Arculus, R., Dale, C., Jenner, F., Pearce, J., et al. (2012). Mantle flow, volatiles, slab-surface temperatures and melting dynamics in the north Tonga arc–Lau back-arc basin. *Journal of Geophysical Research: Solid Earth*, *117*(B11). https://doi.org/10.1029/2012JB009526

Hauri, E., Wang, J., Dixon, J. E., King, P. L., Mandeville, C., & Newman, S. (2002). SIMS analysis of volatiles in silicate glasses: 1. Calibration, matrix effects and comparisons with FTIR. *Chemical Geology*, *183*(1–4), 99–114. https://doi.org/10.1016/S0009-2541(01)00375-8

Helo, C., Longpré, M.-A., Shimizu, N., Clague, D. A., & Stix, J. (2011). Explosive eruptions at mid-ocean ridges driven by CO2-rich magmas. *Nature Geoscience*, *4*(4), 260–263. https://doi.org/10.1038/ngeo1104

Jarosewich, E., Nelen, J. a., & Norberg, J. A. (1980). Reference Samples for Electron Microprobe Analysis*. *Geostandards Newsletter*, *4*(1), 43–47. https://doi.org/10.1111/j.1751-908X.1980.tb00273.x

Jochum, K. P., Stoll, B., Herwig, K., Willbold, M., Hofmann, A. W., Amini, M., et al. (2006). MPI-DING reference glasses for in situ microanalysis: New reference values for element concentrations and isotope ratios. *Geochemistry, Geophysics, Geosystems*, *7*(2). https://doi.org/10.1029/2005GC001060

Kamenetsky, V. S., Everard, J. L., Crawford, A. J., Varne, R., Eggins, S. M., & Lanyon, R. (2000). Enriched End-member of Primitive MORB Melts: Petrology and Geochemistry of Glasses from Macquarie Island (SW Pacific). *Journal of Petrology*, *41*(3), 411–430. https://doi.org/10.1093/petrology/41.3.411

Keller, N. S., Arculus, R. J., Hermann, J., & Richards, S. (2008). Submarine back-arc lava with arc signature: Fonualei Spreading Center, northeast Lau Basin, Tonga. *Journal of Geophysical Research: Solid Earth*, *113*(B8). https://doi.org/10.1029/2007JB005451

Kumamoto, K. M., Warren, J. M., & Hauri, E. H. (2017). New SIMS reference materials for measuring water in upper mantle minerals. *American Mineralogist*, *102*(3), 537–547. https://doi.org/10.2138/am-2017-5863CCBYNCND

Lloyd, A. S., Plank, T., Ruprecht, P., Hauri, E. H., & Rose, W. (2013). Volatile loss from melt inclusions in pyroclasts of differing sizes. *Contributions to Mineralogy and Petrology*, *165*(1), 129–153. https://doi.org/10.1007/s00410-012-0800-2

Mandeville, C. W., Webster, J. D., Rutherford, M. J., Taylor, B. E., Timbal, A., & Faure, K. (2002). Determination of molar absorptivities for infrared absorption bands of H2O in andesitic glasses. *American Mineralogist*, *87*(7), 813–821. https://doi.org/10.2138/am-2002-0702

Mosbah, M., Metrich, N., & Massiot, P. (1991). PIGME fluorine determination using a nuclear microprobe with application to glass inclusions. *Nuclear Instruments and Methods in Physics Research Section B: Beam Interactions with Materials and Atoms*, *58*(2), 227–231. https://doi.org/10.1016/0168-583X(91)95592-2

Newman, S., Stolper, E., & Stern, R. (2000). H2O and CO2 in magmas from the Mariana arc and back arc systems. *Geochemistry, Geophysics, Geosystems*, *1*(5). https://doi.org/10.1029/1999GC000027

Rose-Koga, E. F., Koga, K. T., Devidal, J.-L., Shimizu, N., Voyer, M. L., Dalou, C., & Döbeli, M. (2020). In-situ measurements of magmatic volatile elements, F, S, and Cl, by electron microprobe, secondary ion mass spectrometry, and heavy ion elastic recoil detection analysis. *American Mineralogist*, *105*(5), 616–626. https://doi.org/10.2138/am-2020-7221

Shi, S. C., Towbin, W. H., Plank, T., Barth, A., Rasmussen, D., Moussallam, Y., et al. (2023). PyIRoGlass: An Open-Source, Bayesian MCMC Algorithm for Fitting Baselines to FTIR Spectra of Basaltic-Andesitic Glasses. Retrieved from https://eartharxiv.org/repository/view/6193/

Shimizu, K., Alexander, C. M. O., Hauri, E. H., Sarafian, A. R., Nittler, L. R., Wang, J., et al. (2021). Highly volatile element (H, C, F, Cl, S) abundances and H isotopic compositions in chondrules from carbonaceous and ordinary chondrites. *Geochimica et Cosmochimica Acta*, *301*, 230–258. https://doi.org/10.1016/j.gca.2021.03.005

Shimizu, K., Ushikubo, T., Hamada, M., Itoh, S., Higashi, Y., Takahashi, E., & Ito, M. (2017). H_2O, CO_2, F, S, Cl, and P_2O_5 analyses of silicate glasses using SIMS: Report of volatile standard glasses. *Geochemical Journal*, *51*(4), 299–313. https://doi.org/10.2343/geochemj.2.0470

Shishkina, T. A., Botcharnikov, R. E., Holtz, F., Almeev, R. R., & Portnyagin, M. V. (2010). Solubility of H2O- and CO2-bearing fluids in tholeiitic basalts at pressures up to 500 MPa. *Chemical Geology*, *277*(1–2), 115–125. https://doi.org/10.1016/j.chemgeo.2010.07.014